JBC RESEARCH ARTICLE

Periosteum-derived podoplanin-expressing stromal cells regulate nascent vascularization during epiphyseal marrow development

Received for publication, August 6, 2021, and in revised form, March 8, 2022 Published, Papers in Press, March 15, 2022,
https://doi.org/10.1016/j.jbc.2022.101833

Shogo Tamura[1,*], Masato Mukaide[1], Yumi Katsuragi[1], Wataru Fujii[1], Koya Odaira[1], Nobuaki Suzuki[2], Nagaharu Tsukiji[3], Shuichi Okamoto[4], Atsuo Suzuki[5], Takeshi Kanematsu[4], Akira Katsumi[6], Akira Takagi[7], Katsuhide Ikeda[1], Jun Ueyama[1], Masaaki Hirayama[1], Katsue Suzuki-Inoue[3], Tadashi Matsushita[2,4], Tetsuhito Kojima[1,8], and Fumihiko Hayakawa[1]

From the [1]Department of Integrated Health Sciences, Nagoya University Graduate School of Medicine, Nagoya, Japan; [2]Department of Transfusion Medicine, Nagoya University Hospital, Nagoya, Japan; [3]Department of Clinical and Laboratory Medicine, Faculty of Medicine, University of Yamanashi, Chuo, Yamanashi, Japan; [4]Department of Clinical Laboratory, Nagoya University Hospital, Nagoya, Japan; [5]Department of Medical Technique, Nagoya University Hospital, and [6]Department of Hematology, National Center for Geriatrics and Gerontology, Obu City, Japan; [7]Department of Medical Technology, Shubun University, Ichinomiya, Japan; [8]Aichi Health Promotion Foundation, Nagoya, Japan

Edited by Qi-Qun Tang

Bone marrow development and endochondral bone formation occur simultaneously. During endochondral ossification, periosteal vasculatures and stromal progenitors invade the primary avascular cartilaginous anlage, which induces primitive marrow development. We previously determined that bone marrow podoplanin (PDPN)-expressing stromal cells exist in the perivascular microenvironment and promote megakaryopoiesis and erythropoiesis. In this study, we aimed to examine the involvement of PDPN-expressing stromal cells in postnatal bone marrow generation. Using histological analysis, we observed that periosteum-derived PDPN-expressing stromal cells infiltrated the cartilaginous anlage of the postnatal epiphysis and populated on the primitive vasculature of secondary ossification center. Furthermore, immunophenotyping and cellular characteristic analyses indicated that the PDPN-expressing stromal cells constituted a subpopulation of the skeletal stem cell lineage. *In vitro* xenovascular model cocultured with human umbilical vein endothelial cells and PDPN-expressing skeletal stem cell progenies showed that PDPN-expressing stromal cells maintained vascular integrity *via* the release of angiogenic factors and vascular basement membrane-related extracellular matrices. We show that in this process, Notch signal activation committed the PDPN-expressing stromal cells into a dominant state with basement membrane-related extracellular matrices, especially type IV collagens. Our findings suggest that the PDPN-expressing stromal cells regulate the integrity of the primitive vasculatures in the epiphyseal nascent marrow. To the best of our knowledge, this is the first study to comprehensively examine how PDPN-expressing stromal cells contribute to marrow development and homeostasis.

The bone marrow is a three-dimensional tissue within the bone cavity that is composed of the vasculature, extracellular matrices (ECMs), and stromal cells (1, 2). Bone marrow development and bone formation occur simultaneously. In mammals, bones are formed *via* two distinct mechanisms, that is, intramembranous and endochondral ossification. Intramembranous ossification is the process of bone development from soft connective tissue that is involved in the formation of flat bones of the skull (calvarial bones and mandibles) and part of the clavicles. Endochondral ossification is the process of bone development from cartilage that forms all bones of the body, except the flat bones of the skull. During the endochondral ossification, the vascular invasion of the primary avascular cartilaginous anlage triggers the formation of an embryonal primary ossification center (POC) and postnatal secondary ossification center (SOC) in the diaphysis and epiphysis, respectively (3). The invading vasculature transports chondroclasts, osteoblast progenitors, and stromal progenitors from the periosteum to the POC or SOC (4, 5). The invading vasculature and stromal progenitors generate the primitive marrow inside the bone cavity.

Skeletal stem cells (SSCs) are a heterogenous population of stromal cells that play a role in bone marrow generation, skeletal tissue development, homeostasis, and regeneration (6, 7). In mice, SSCs exist within the periosteum (8–11), bone marrow (BM-SSCs, also known as bone marrow stem/stromal cells, BMSCs) (12–23), and growth plate resting zone (24, 25). Studies involving mouse BM-SSCs have identified several BM-SSC subpopulations [*e.g.*, CXCL12 abundant reticular cells (12–15), leptin receptor-positive cells (16–18), *nestin*^{GFP}-positive cells (21, 22), *grem1*$^{Cre\text{-}ERT}$-positive cells (20), and Mx1-positive cells (11, 19)]. These BM-SSC subsets are present at the abluminal surface of blood vessels and induce the formation of hematopoietic microenvironments *via* the expression of hematopoietic regulators, such as CXCL12 and SCF (26, 27).

* For correspondence: Shogo Tamura, stamura@met.nagoya-u.ac.jp.

Previously, we have identified podoplanin (PDPN, also known as gp38 or T1a)-expressing stromal cells that existed in the bone marrow (28). In adult mice, PDPN-expressing stromal cells induce the generation of a perivascular microenvironment that promotes megakaryopoiesis and erythropoiesis (28, 29). However, the cellular sources and physiological functions of PDPN-expressing stromal cells during postnatal bone marrow development have not been elucidated.

This study is to characterize the cellular features of marrow PDPN-expressing stromal cells and disclose how these cells are involved in the postnatal bone marrow generation. To the best of our knowledge, this is the first study to investigate the role of PDPN-expressing stromal cells on marrow development and homeostasis. These findings will improve our understanding of how stromal cells regulate nascent bone marrow development and homeostasis.

Results

PDPN-expressing periosteal cells invade into the postnatal primary epiphysis and are present in primitive vascular beds

We and other research group (Baccin C *et al*) had previously detected PDPN-expressing stromal cells in the diaphyseal marrow of adult mice (>8-week old) (28, 30). In this study, to investigate the source of PDPN-expressing stromal cells and their physiological functions in the postnatal nascent bone marrow, we attempted to screen their distribution in mice femurs at postnatal day 21 (P21). Since the number of PDPN-expressing stromal cells in the marrow was very low, we enriched PDPN-positive marrow cells using magnetic microbeads (Fig. 1*A*). Using flow cytometric analysis, we detected the PDPN-expressing stromal cells in the diaphyseal and epiphyseal marrow (Fig. 1*B*). In the stromal population of the PDPN-positive enriched marrow [Lin(-)CD31(-)CD45(-)CD51(+)CD150(-)], more PDPN-expressing stromal cells were detected in the epiphysis than in the diaphysis. The diaphyseal PDPN-expressing stromal cells were stem cell antigen-1 (Sca-1)-negative; these findings were consistent with those of our previous study (28). In contrast, the epiphyseal PDPN-expressing stromal cells were mainly Sca-1 positive. These data indicate the characteristic differences between the epiphyseal and diaphyseal PDPN-expressing stromal cells. To analyze these newly identified cells, we evaluated the epiphyseal marrow using histological analysis. At P21—in the cryosection of the epiphysis—PDPN-expressing stromal cells were detected in the SOC and surrounding primitive vasculatures (Fig. 1*C*). Upon evaluating the expression of pericyte markers, platelet-derived growth factor receptor β (PDGFRβ), neuron-glial antigen 2 (NG2), and alpha smooth muscle actin (αSMA) (31), in these cells, we observed that the epiphyseal marrow PDPN-expressing stromal cells were PDGFRβ positive, NG2 positive, and αSMA negative (Fig. 1, *D*–*F*). The pericytes, determined to be PDGFRβ(+)NG2(+)αSMA(-), are generally observed on the capillary bed (32). These findings suggest that epiphyseal PDPN-expressing stromal cells can act as pericytes in primitive capillary-like vascular beds in the developing SOC.

Next, we investigated how PDPN-expressing stromal cells populated the epiphyseal marrow. We sequentially chased epiphyseal SOC development from P7 to P14 (Fig. 2). At P7, the periosteal artery invaded into the epiphysis. At this time, PDPN-expressing cells were mainly observed within the periosteum, and some were detected within the vascular tip penetrating the epiphyseal cartilaginous anlage (Fig. 2*A*). SOC formation and vascularization were initiated at P9. During this process, PDPN-expressing stromal cells began to associate with vascular endothelial cells (Fig. 2*B*). The SOC became highly vascularized from P10 to P14. PDPN-expressing stromal cells were widely infiltrated in the SOC and present in the primitive vasculature (Fig. 2, *C*–*G*). Moreover, during SOC formation, the proliferative expansion of these cells occurred at the penetrating tip of the periosteum (Fig. S1). These findings suggest that epiphyseal PDPN-expressing stromal cells originate from the periosteal cellular component, populate the epiphyseal SOC, and behave as pericytes.

Epiphyseal PDPN-expressing stromal cells are subpopulation of the SSC lineage

To clarify the cellular characteristics of epiphyseal PDPN-expressing stromal cells, we investigated their potential to act as SSCs. Chan *et al*. established a flow cytometric strategy to fractionate SSCs [Lin(-)CD31(-)CD45(-)CD51(+)CD90(-)CD249(-)CD200(+)CD105(-)] and SSC-lineage progenitors [pre-bone cartilage stroma progenitors (pre-BCSPs), Lin(-)CD31(-)CD45(-)CD51(+)CD90(-)CD249(-)CD200(-)CD105(-)] (25). We used this strategy to investigate whether epiphyseal PDPN-expressing stromal cells are detected in the SSC or pre-BCSP fractions. The flow cytometric analysis detected a minor population of epiphyseal PDPN-expressing stromal cells in SSCs and pre-BCSPs (Fig. 3, *A* and *B*). The percentages of PDPN-expressing stromal cells in each fraction were 0.202 ± 0.020% and 2.189 ± 0.309% in the SSCs and pre-BCSPs, respectively (Fig. 3*C*). The colony formation assay revealed that the clonogenicity of the epiphyseal PDPN-expressing stromal cells was significantly lower than that of primary SSCs and pre-BCSPs (Fig. 3*D*). *In vitro* osteo/adipo/chondrogenic differentiation assays showed that PDPN-expressing stromal cells had the potential to differentiate into osteoblast, adipocyte, and chondrocyte; however, their chondrogenicity was less capable than that of the SSCs (Fig. 3*E*). We further evaluated their gene expression of *Sp7*, a transcriptional factor regulating osteoblast differentiation, *Pparg*, a transcriptional factor regulating differentiation into adipocytes, and *Acan*, a proteoglycan that was highly expressed in chondrocytes. In the osteogenic and adipogenic differentiations, the PDPN-expressing stromal cells showed comparable gene expression levels of *Sp7* and *Pparg* to those of SSCs (Fig. 3, *F* and *G*). In the chondrogenic differentiation, the expression of *Acan* in the PDPN-expressing stromal cells was significantly lower than that of SSCs (Fig. 3*H*). These findings suggest that the epiphyseal PDPN-expressing stromal cells present different cellular characteristics compared to those of SSCs.

To investigate their cell lineage, we cultured the primary SSCs with MesenCult and observed the PDPN expression levels. In

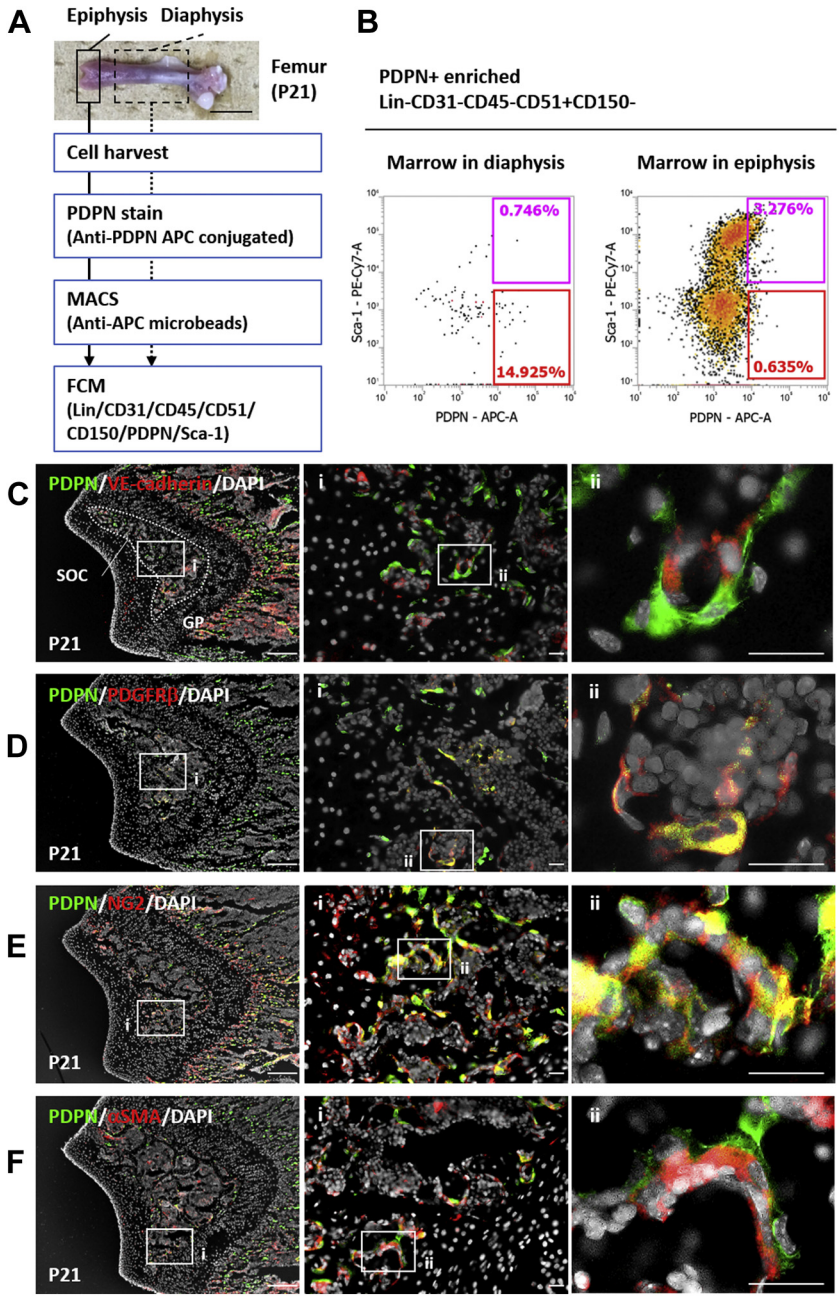

Figure 1. Epiphyseal PDPN-expressing stromal cells are the pericytes on the primitive capillary-like vascular bed of the secondary ossification center. *A*, scheme to detect marrow PDPN-expressing stromal cells *via* flow cytometry. The scale bar indicates 5 mm. *B*, representative flow cytometric data of PDPN-expressing stromal marrow cells in the epiphysis and diaphysis in mice at P21. PDPN-positive enriched marrow cells were analyzed by flow cytometry. *Magenta* and *red* gates indicate the PDPN(+)/Sca-1(+) and PDPN(+)/Sca-1(-) populations, respectively. The percentages inside each gate indicate the cells contained in the population of Lin(-)CD31(-)CD45(-)CD51(+)CD150(-). *C*, representative IHC images of P21 mouse epiphysis. Epiphysis cryo-sections were stained with PDPN, VE-cadherin, and DAPI. PDPN-expressing stromal cells surrounded primitive vasculatures. *D–F*, representative IHC images of P21 mouse epiphysis with PDPN/PDGFRβ/DAPI (D), PDPN/NG2/DAPI (*E*), and PDPN/αSMA/DAPI (*F*). Scale bars in the *left* indicate 200 μm. Scale bars in the *middle* and *right* panels indicate 50 μm. αSMA, α-smooth muscle actin; DAPI, 4′,6-diamidino-2-phenylindole, IHC, immunohistochemistry; NG2, neuron-glial antigen-2, P21, postnatal day 21, PDPN, podoplanin, PDGFRβ, platelet-derived growth factor receptor-β, Sca1, stem cell antigen-1, VE-cadherin, vascular endothelial-cadherin.

this experiment, primary SSCs were isolated from the epiphysis at P21, which probably contained periosteal SSCs as a major fraction and growth plate resisting zone-SSCs as a minor fraction. During their culture with MesenCult, epiphyseal primary SSCs differentiated into skeletal lineage progenitors, including pre-BCSPs (CD51+CD90-CD249-CD200-CD105-), BCSPs (CD51+CD90-CD249-CD200-CD105+), osteo/chondrogenic progenitors (CD51+CD90+), and stromal cells (CD51+CD90-CD249+) (Fig. 4*A*). These *in vitro*-differentiated SSC progenies expressed PDPN and Sca-1 at high levels (Fig. 4*B*). To characterize the PDPN-expressing SSC progenies *in vitro*, we further investigated their surface markers and compared them with those of epiphyseal PDPN-expressing stromal cells. Immunocytochemistry (ICC) showed that PDPN-expressing

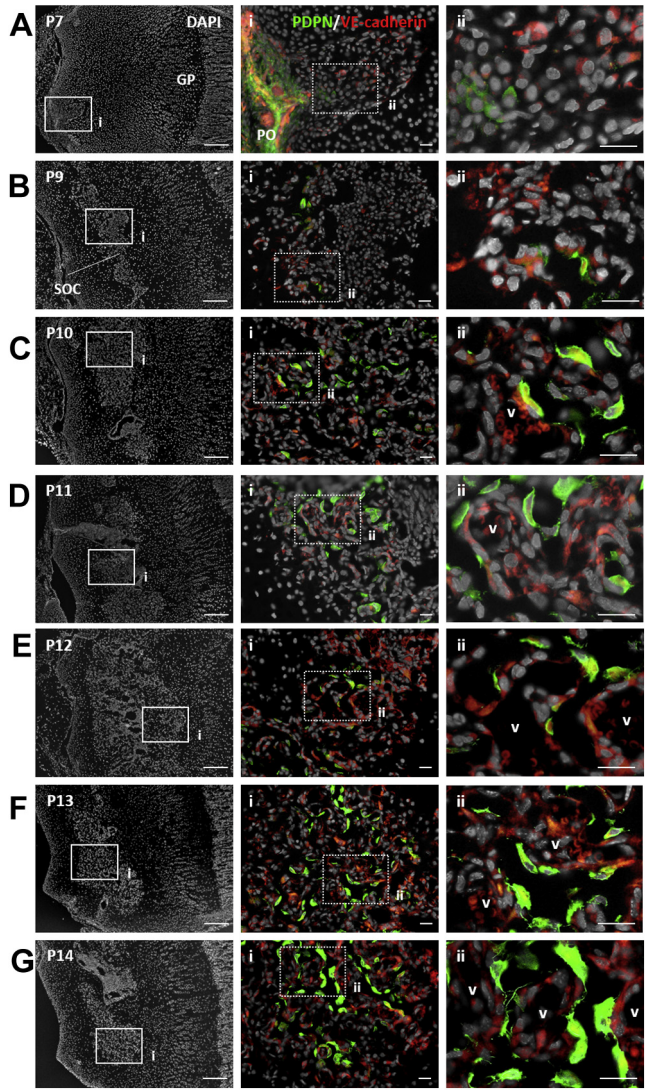

Figure 2. Epiphyseal PDPN-expressing stromal cells originate from the periosteal cellular component and populate the secondary ossification center as pericytes. *A–G*, representative IHC images of postnatal mouse epiphysis at P7 (*A*), P9 (*B*), P10 (*C*), P11 (*D*), P12 (*E*), P13(*F*), and P14 (*G*). Epiphysis cryo-sections were stained with PDPN, VE-cadherin, and DAPI. Scale bars in the *left* indicate 200 μm. Scale bars in the *middle* and *right* panels indicate 50 μm. DAPI, 4′,6-diamidino-2-phenylindole; IHC, immunohistochemistry; PDPN, podoplanin; P7, P9, P10, P11, P12, P13, P14, postnatal day 7, 9, 10, 11, 12, 13, 14; VE-cadherin, vascular endothelial-cadherin.

SSC progenies expressed PDGFRβ and NG2, but not αSMA (Fig. 4, *C–E*), and exhibited a surface marker pattern observed in epiphyseal PDPN-expressing stromal cells (Fig. 1, *D–F*). These observations suggest that epiphyseal PDPN-expressing stromal cells are subpopulation of the SSC lineage.

PDPN-expressing SSC progenies maintain the HUVEC lumens via *the release of angiogenic factors in the xenovascular model*

Since epiphyseal PDPN-expressing stromal cells were present on the primitive vascular beds in the SOC *in vivo*, we hypothesized that these cells could regulate vascular integrity and/or marrow homeostasis. To verify this hypothesis, we used *in vitro* PDPN-expressing SSC progenies as a cellular model of *in vivo* epiphyseal PDPN-expressing stromal cells. In addition, we established a xenovascular model by coculturing human umbilical vein endothelial cells (HUVECs) with *in vitro* PDPN-expressing SSC progenies. In the xenovascular model, non-endothelial cells with fibroblastic morphologies were attached to HUVEC vascular-like cords (Fig. 5*A*). ICC revealed that these pericyte-like cells expressed PDPN, PDGFRβ, and NG2, but not vascular endothelial (VE)-cadherin (Fig. 5, *B–D*). These observations indicate that *in vitro* PDPN-expressing SSC progenies behave as pericytes surrounding the HUVEC cords and mimicked epiphyseal PDPN-expressing stromal cells presented on the primitive vascular beds in the SOC. Next, we investigated whether SSC progenies–expressing PDPN *in vitro* maintained HUVEC lumens. Compared to the conditions used for the monoculture of HUVECs, the parameters used to evaluate HUVEC lumen integrity (*i.e.*, the number of junctions, the number of segments, the number of meshes, and the total mesh area) were significantly maintained in the xenovascular model. (Fig. 5,*E–I*). Moreover, the luminal regulation of PDPN-expressing SSC progenies was sustained for at least 6 days (Fig. S2). These observations indicate that PDPN-expressing SSC progenies consolidate the HUVEC lumens *in vitro*.

To investigate the mechanism of vascular regulation by *in vitro* PDPN-expressing SSC progenies, we analyzed soluble factors in a conditioned medium derived from PDPN-expressing SSC progenies (SSC-progeny CM). The HUVEC proliferation assay showed that SSC-progeny CM significantly accelerated cell proliferation (Fig. 6*A*). This proliferative activity was much higher than that of the commercially available endothelial cell growing medium (EGM2). Scratch assays revealed that SSC-progeny CM also facilitated HUVEC migration (Fig. 6*B*). Therefore, we investigated whether SSC-progeny CM consolidated the HUVEC lumens. When compared to the nonconditioned medium (Non-CM), the SSC-progeny CM significantly enabled the parameters required for HUVEC lumen integrity to be maintained (Fig. 6, *C–G*); this mimicked the behavior in the xenovascular model containing HUVECs and PDPN-expressing SSC progenies (Fig. 5,*E–I*). To profile the soluble factors regulating HUVEC lumen integrity, we performed a protein array analysis of 53 angiogenesis-related factors. The results revealed that SSC-progeny CM contained various angiogenic factors, and the spot intensities of eight angiogenic factors, that is, IGFBP-2 (33), osteopontin (34), CCL2 (35), MMP-3 (36, 37), CXCL12 (38), PAI-1 (39–41), TSP-2 (42, 43), and vascular endothelial growth factor-A (VEGF-A), were particularly increased (Figs. 6*H* and S3). Since VEGF-A is a major angiogenic factor, we investigated whether VEGF inhibition influenced HUVEC neovascularization in culture with SSC-progeny CM. In this experiment, we blocked VEGF-A–vascular endothelial growth factor receptor (VEGFR2) interaction by neutralizing antibodies against VEGF-A or VEGFR2. HUVEC tube formation assay revealed that the blockage of VEGF-A–VEGFR2 interaction suppressed the early phase lumen construction with SSC-progeny CM; however, their HUVEC lumen integrities were still mostly retained (Fig. S4). These data indicate that

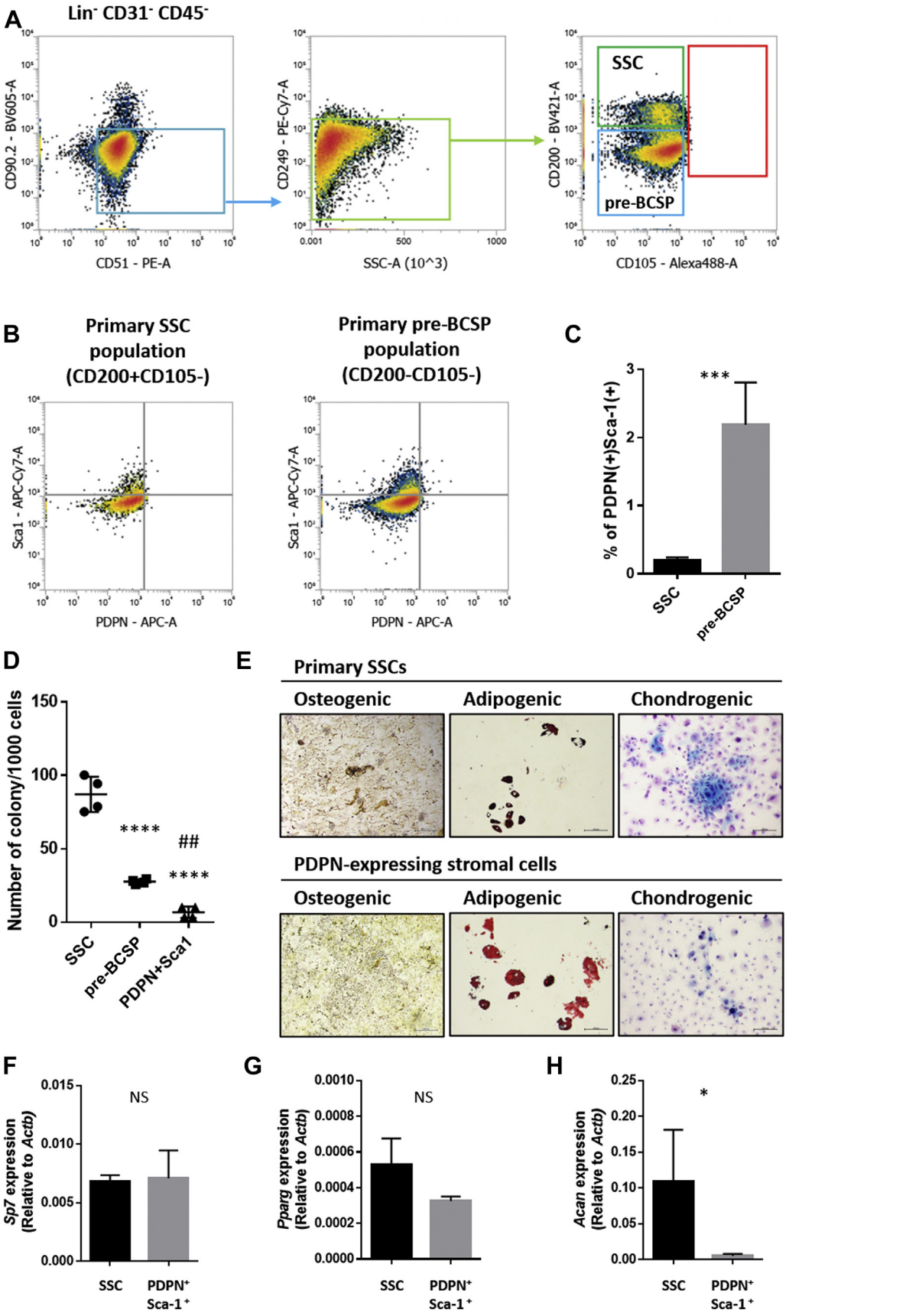

Figure 3. Epiphyseal PDPN-expressing stromal cells partially exhibit the SSC lineage phenotype. *A*, flow cytometric gating strategy for the mouse epiphyseal skeletal stem cell lineage. Cells that were Lin(-)CD31(-)CD45(-)CD51(+)CD90(-)CD249(-)CD200(+)CD105(-) were identified as SSCs. Cells that were Lin(-)CD31(-)CD45(-)CD51(+)CD90(-)CD249(-)CD200(-)CD105(-) were identified as SSC-lineage progenitor and pre-BCSP populations. *B*, representative flow

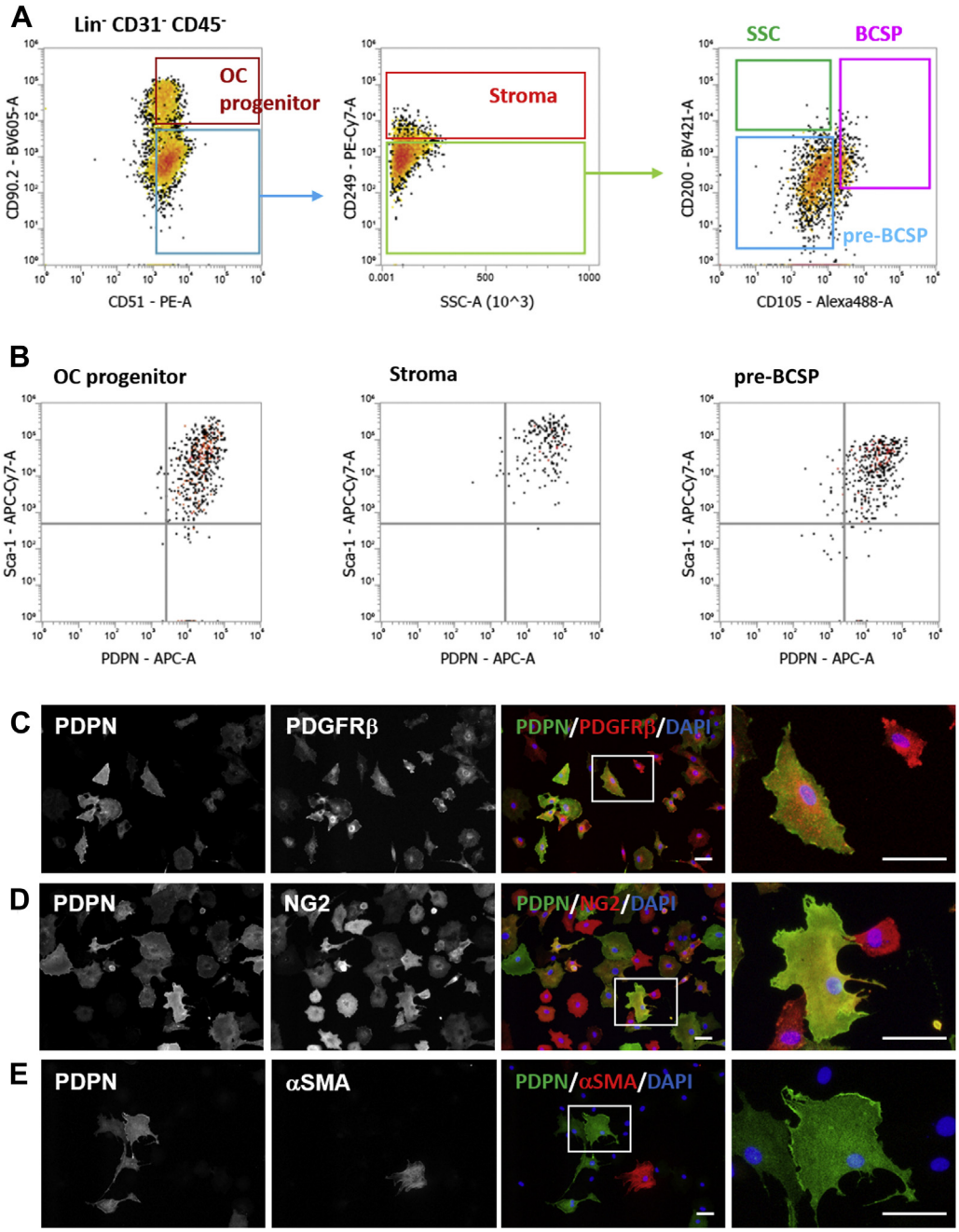

Figure 4. SSCs generate PDPN-expressing progenies with a phenotype identical to that of epiphyseal PDPN-expressing stromal cells. *A*, representative flow cytometric data of *in vitro* SSC progenies generated from primary isolated SSCs during culture with MesenCult. *B*, PDPN and Sca-1 expression in *in vitro* generated SSC progenies. *C–E*, representative ICC images of the *in vitro* PDPN-expressing SSC progenies stained with PDPN/PDGFRβ/DAPI (*C*), PDPN/NG2/DAPI (*D*), and PDPN/αSMA/DAPI (*E*). Scale bars indicate 50 μm. αSMA, α-smooth muscle actin; DAPI, 4′,6-diamidino-2-phenylindole; ICC, immunocytochemistry; NG2, neuron-glial antigen-2; PDGFRβ, platelet-derived growth factor receptor-β; Sca-1, stem cell antigen-1; PDPN, podoplanin; SSC, skeletal stem cell.

cytometric scattergrams detecting the PDPN-expressing stromal cells in the epiphyseal primary SSC and pre-BCSP populations. *C*, quantitative data of the PDPN-expressing stromal cells in the epiphyseal primary SSC and pre-BCSP populations. ***$p < 0.001$, as detected by the Student's *t* test (n = 4 per group); the error bars represent SDMs. *D*, colony formation assay analyzing the clonogenicity of epiphyseal PDPN-expressing stromal cells. Primary SSCs, pre-BCSPs, and PDPN-expressing stromal cells in the epiphysis were isolated using the cell sorter, and 1000 cells/well were seeded into a 24-well plate. Colonies were counted *via* Giemsa staining. ****$p < 0.0001$ *versus* SSCs. ##$p < 0.01$ *versus* pre-BCSPs. Statistical analysis was performed using one-way ANOVA with Tukey's multiple comparison test (n = 4 per group). The error bars represent SDMs. *E*, osteo/adipo/chondrogenic differentiation ability of epiphyseal PDPN-expressing stromal cells. The differentiation of osteogenic, adipogenic, and chondrogenic lineages was evaluated *via* Von Kossa staining (*black*/*brown*), Oil-red staining (*red*), and Alcian blue staining (*sky-blue*), respectively. Scale bars indicate 200 μm. *F–H*, RT-qPCR evaluating the expression of the genes encoding proteins that regulate osteo/adipo/chondrogenic differentiation. The gene expression levels of *Sp7* (*F*), *Pparg* (*G*), and *Acan* (*H*) were assessed at differentiation day 12. *$p < 0.05$. Statistical analysis was performed by Mann-Whitney U-test (n = 4 per group) PDPN, podoplanin; pre-BCSP, pre-bone cartilage stroma progenitor; RT-qPCR, reverse transcribed-quantitative PCR; SDMs, mean ± standard deviation values of the mean; SSC, skeletal stem cell.

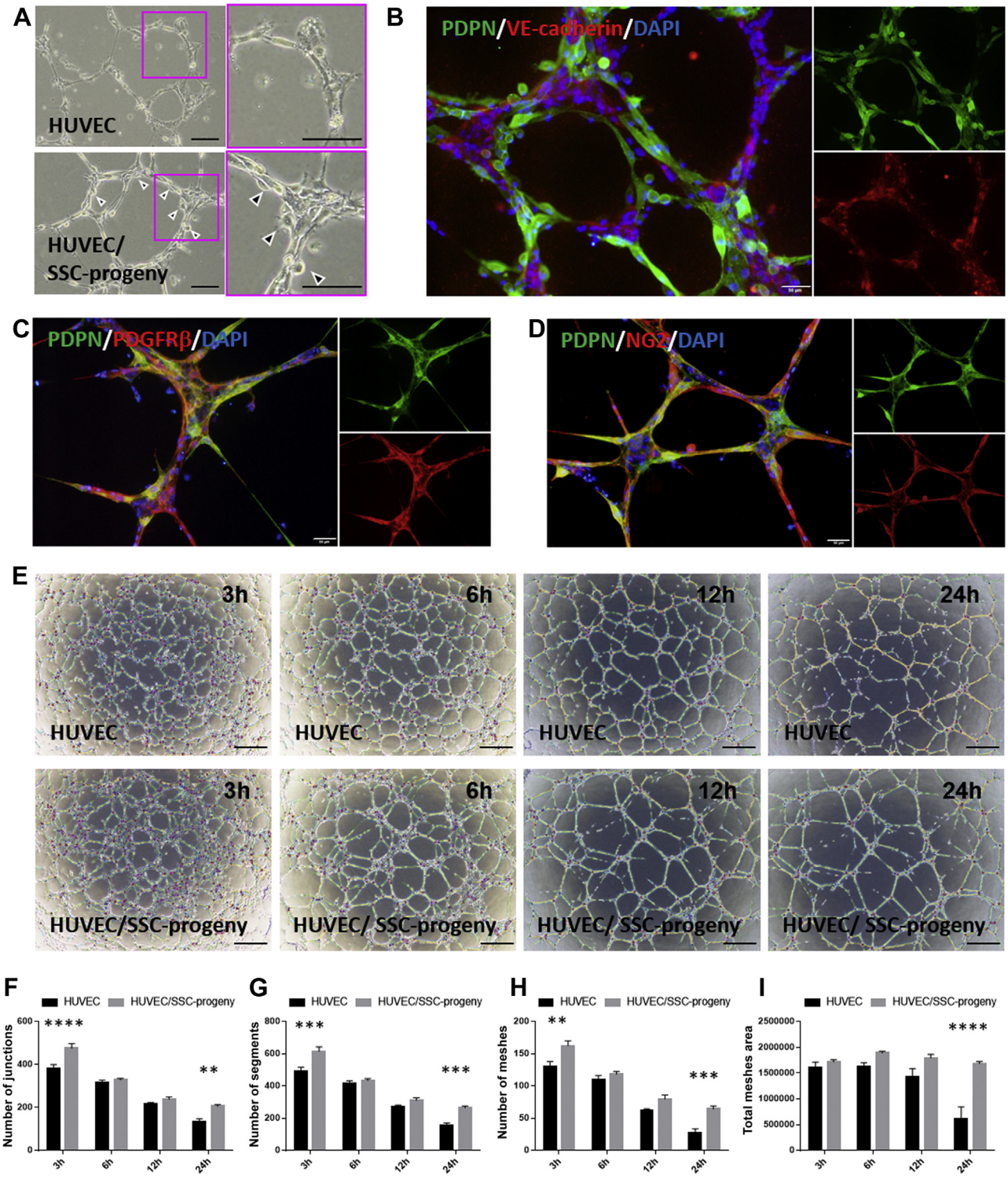

Figure 5. *In vitro* PDPN-expressing SSC progenies consolidate HUVEC capillary-like lumens in a xenovascular model. *A*, representative optical microscope images of the vascular-like lumen of HUVECs (*upper* panel) and the xenovascular model cocultured with HUVECs and PDPN-expressing SSC progenies *in vitro* (*lower* panel). *Arrow heads* indicate nonendothelial cells with fibroblastic morphologies attached onto HUVEC cords. Scale bar indicates 100 μm. *B*, representative ICC images of the xenovascular model stained with PDPN, VE-cadherin, and DAPI. Scale bar indicates 50 μm. *C* and *D*, representative ICC images of the xenovascular images stained with PDPN/PDGFRβ/DAPI (*C*) and PDPN/NG2/DAPI (*D*). Scale bars indicate 50 μm. *E*, time series images of HUVEC vascular-like lumens (upper panels) and the xenovascular models cocultured with HUVECs and PDPN-expressing SSC progenies *in vitro* (*lower panels*). The time displayed on each image indicates the time point at the start of the culture process. Scale bar indicates 500 μm. *F–I*, quantitative analysis of vascular lumen integrity in the xenovascular model. The parameters used to evaluate lumen vascularization, including the number of junctions (*F*), the number of segments (*G*), the number of meshes (*H*), and the total mesh area (*I*), were measured using the angiogenesis analyzer tool. $^{**}p < 0.01$. $^{***}p < 0.001$. $^{****}p < 0.0001$. Statistical analysis was performed *via* two-way ANOVA and Sidak's multiple comparison test (n = 5 per group). The error bars represent SEMs. DAPI, 4′,6-diamidino-2-phenylindole; HUVEC, human umbilical vein endothelial cell; ICC, immunocytochemistry; NG2, neuron-glial antigen-2; PDPN, podoplanin; PDGFRβ, platelet-derived growth factor receptor-β; SSC, skeletal stem cell; SEMs, mean ± standard error values of the mean; VE-cadherin, vascular endothelial-cadherin.

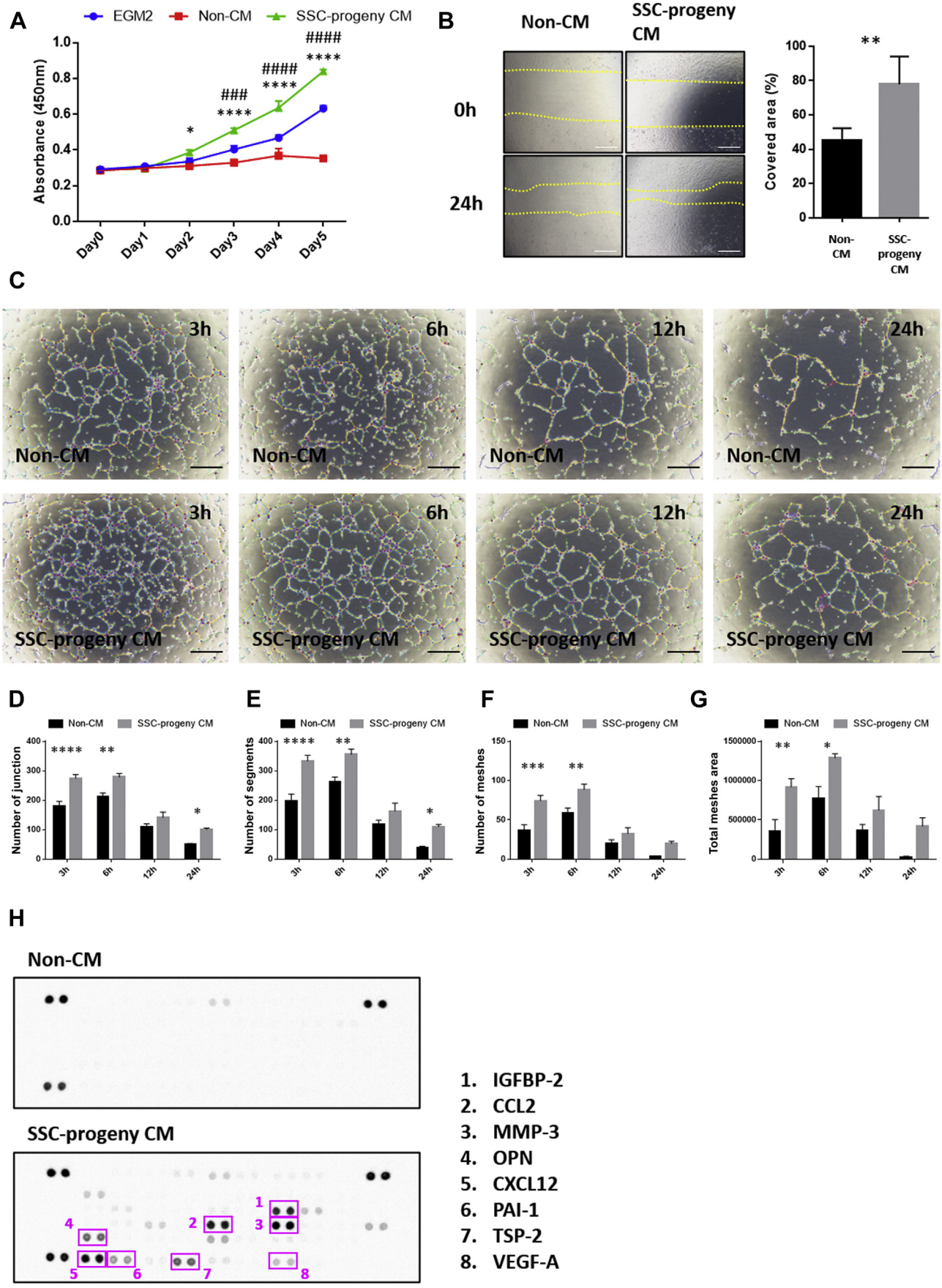
A
EGM2
Non-CM
SSC-progeny CM
Absorbance (450nm)
Day0
Day1
Day2
Day3
Day4
Day5
B
Non-CM
SSC-progeny CM
0h
24h
Covered area (%)
Non-CM
SSC-progeny CM
C
3h
6h
12h
24h
Non-CM
SSC-progeny CM
D
Number of junction
E
Number of segments
F
Number of meshes
G
Total meshes area
H
Non-CM
SSC-progeny CM
1. IGFBP-2
2. CCL2
3. MMP-3
4. OPN
5. CXCL12
6. PAI-1
7. TSP-2
8. VEGF-A

PDPN-expressing SSC progenies autonomously secrete various angiogenic factors that maintain HUVEC lumens in concert. Thus, we suggest that epiphyseal PDPN-expressing stromal cells positively regulate the integrity of the primitive vasculature, *via* the release of angiogenic factors.

PDPN-expressing SSC progenies secrete components of the basement membrane matrices in interaction with HUVECs

Vascular integrity is maintained by not only endothelial cell survival, but also by the microenvironments in the perivascular space. ECM is one of the major environmental factors secreted by endothelial cells and their pericytes that maintain vascular homeostasis (44, 45). We investigated whether *in vitro* PDPN-expressing SSC progenies secrete collagenous and non-collagenous ECM components. First, we determined the expression of type IV collagen and laminin isoforms in *in vitro* PDPN-expressing SSC progenies under monoculture conditions (Fig. 7, *A* and *B*). The *in vitro* PDPN-expressing SSC progenies endogenously produce type IV collagen and laminin; however, the extracellular deposition of these ECMs was not observed. Second, we analyzed the extracellular deposition of basement membrane ECMs in the xenovascular model (Fig. 7, *C–F*). The extensive deposition of type IV collagen and laminin isoforms was observed in close proximity to the luminal cords (Fig. 7, *C* and *E*). Quantitative image analysis showed that the levels of the deposited type IV collagen and laminin isoforms were significantly increased during the coculture of HUVECs with *in vitro* PDPN-expressing SSC progenies, compared to the levels observed in HUVEC monoculture (Fig. 7, *D* and *F*). These findings indicate that interactions with HUVECs induce *in vitro* PDPN-expressing SSC progenies to secrete ECMs in the periluminal space.

Cell–cell interaction with HUVECs switches the phenotype of PDPN-expressing SSC progenies to basement membrane-related gene dominant state

Next, we examined whether the cell–cell interactions with HUVECs altered the ECM transcript pattern of PDPN-expressing SSC progenies. Xenovascular capillaries were enzymatically dissociated, and co-cultured PDPN-expressing SSC progenies were isolated *in vitro via* cell sorting (Fig. 8*A*). After immunostaining with anti-mouse PDPN-APC and anti-human CD31-FITC antibodies, PDPN-expressing SSC progenies were identified to be mouse PDPN-positive/human CD31-negative cells (Fig. 8*B*). Reverse transcribed-quantitative PCR revealed that the transcript expression level of mouse vascular basement membrane-related collagenous ECM genes, that is, type IV collagen alpha-chains (*Col4a1* and *Col4a2*), in PDPN-expressing SSC progenies was significantly upregulated upon coculture with HUVECs (Fig. 8, *C* and *D*). We evaluated the expression of genes related to non-collagenous basement membrane ECMs, such as laminin alpha-chains (*Lama4* and *Lama5*) and nidogen isoforms (*Nid1* and *Nid2*) (Fig. 8, *E–H*). Among these noncollagenous ECM-related genes, the expression of *lama5* and *Nid1* was significantly upregulated in PDPN-expressing SSC progenies upon coculture with HUVECs, whereas the expression of *Lama4* was not altered and that of *Nid2* was significantly decreased. However, the expression of genes encoding non-basement membrane fibrillar collagen, that is, *Col1a1* and *Col3a1*, was downregulated in PDPN-expressing SSC progenies and remained unaltered after coculture with HUVECs (Fig. 8,*I* and *J*). These findings show that the interaction of PDPN-expressing SSC progenies with HUVECs causes switching the phenotype of PDPN-expressing SSC progenies to the basement-membrane–dominant state.

Notch pathway activation upregulates gene expression of basement membrane-related collagenous ECMs in PDPN-expressing SSC progenies

Notch activation reportedly upregulated the expression of basement membrane ECM-related genes in BM-SSCs *in vivo* (46). We pharmacologically investigated whether Notch signals were responsible for alterations in the ECM phenotype of PDPN-expressing SSC progenies *in vitro*. To inhibit the Notch pathway, we treated PDPN-expressing SSC progenies with LY-411575, a Notch pathway inhibitor, in the background of coculture with HUVECs and evaluated their ECM-related gene expression levels (Fig. 9*A*). LY-411575 did not affect the morphology and vascular integrity of the xenovascular model (Fig. S5). Notch pathway inhibition significantly suppressed the HUVEC-induced upregulation of *Col4a1*, *Col4a2*, *Lama5*, and *Nid1* (Fig. 9, *B–E*), but did not affect *Nid2* expression level in the background of HUVEC coculture (Fig. 9*F*).

We further investigated the Notch involvement in the phenotype switching of PDPN-expressing SSC progenies by a molecular approach using recombinant Notch ligands. HUVECs express four types of Notch ligands: Jagged1 (JAG1),

Figure 6. PDPN-expressing SSC progenies autonomously release various angiogenic factors that coordinate with each other to maintain HUVEC lumens *in vitro*. *A*, HUVEC proliferation assay. HUVECs were cultured with the EGM2, non-CM, and SSC-progeny CM media. HUVEC proliferation was assessed *via* the WST-8 assay. *$p < 0.05$ *versus* Non-CM. ****$p < 0.0001$ *versus* Non-CM. ###$p < 0.001$ *versus* EGM2. ####$p < 0.0001$ *versus* EGM2. Statistical analysis was performed using two-way ANOVA and Sidak's multiple comparison test (n = 3 per group). The error bars represent SEMs. *B*, HUVEC scratch assay. The panel on the *left* indicates the representative optical microscopic images of scratched HUVEC monolayers cultured with non-CM and SSC-progeny CM media at 0 h or 24 h. The panel on the *right* indicates the quantitative data of the covered area, 24 h after culturing cells with non-CM and SSC-progeny CM media. **$p < 0.01$, as detected by the Student's *t* test (n = 5 per group). Scale bars indicate 200 μm. *C*, time series images of HUVEC vascular-like lumens in non-CM (*upper* panels) and SSC-progeny CM (*lower* panels) media. Scale bar indicates 500 μm. *D–G*, quantitative analysis of HUVEC vascular lumen integrity using non-CM or SSC-progeny CM media. The parameters used for evaluating lumen vascularization, including the number of junctions (*D*), the number of segments (*E*), the number of meshes (*F*), and the total mesh area (*G*), were measured using the angiogenesis analyzer tool. *$p < 0.05$. **$p < 0.01$. ***$p < 0.001$. ****$p < 0.0001$. Statistical analysis was performed by two-way ANOVA and Sidak's multiple comparison test (n = 5 per group). The error bars represent SEMs. *H*, profiling the soluble factors to regulate HUVEC lumen integrity in the SSC-progeny CM medium. The soluble factors were profiled by using the Proteome Profiler Mouse Angiogenesis Array Kit. The *top* and *bottom* panels indicate the array images generated with non-CM and SSC-progeny CM media, respectively. PDPN, podoplanin; SSC, skeletal stem cell; HUVEC, human umbilical vein endothelial cell; EGM2, endothelial growth medium-2; non-CM, EGM2-basal medium supplemented with non-conditioned medium; SSC-progeny CM, EGM2-basal medium supplemented with *in vitro* PDPN-expressing SSC-progeny conditioned medium.

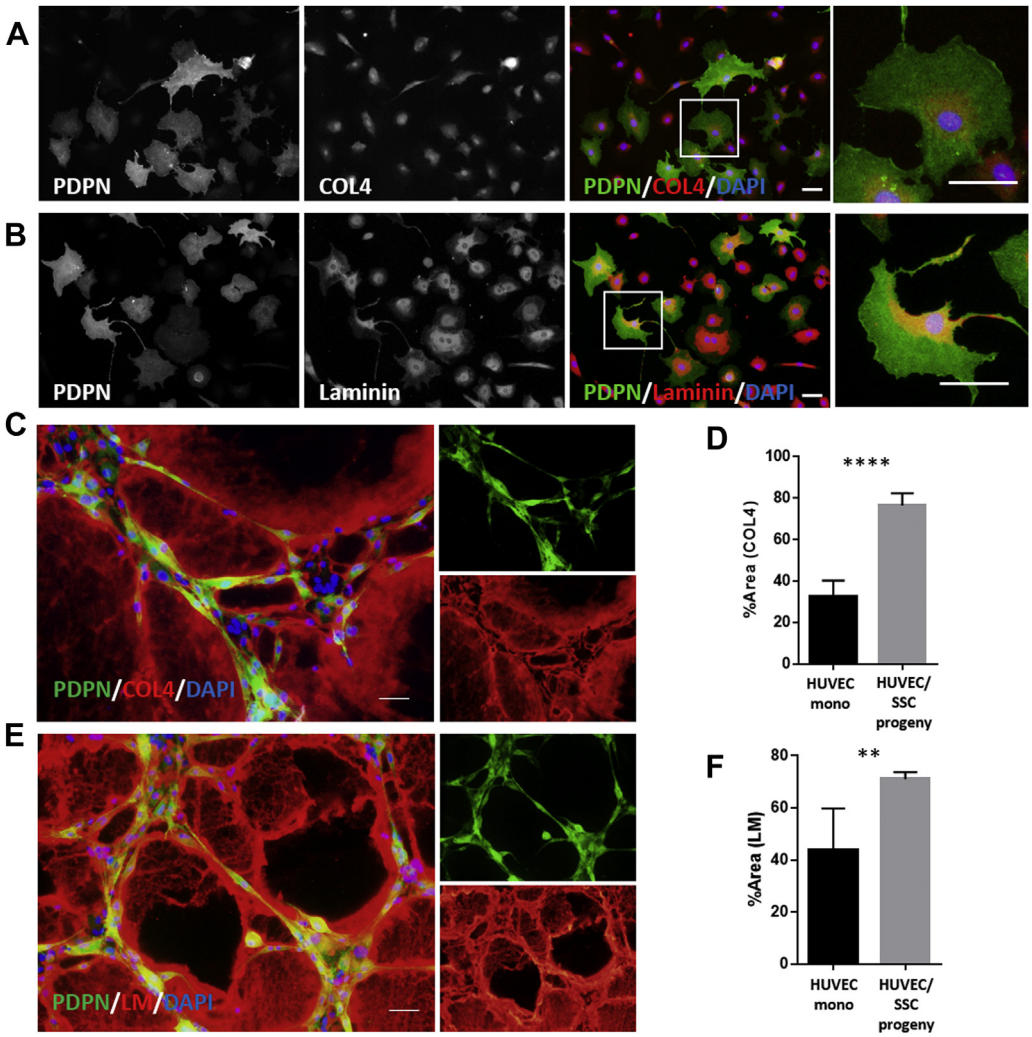

Figure 7. Cell–cell interactions with HUVECs induce PDPN-expressing SSC progenies to release ECMs in the periluminal space *in vitro*. *A* and *B*, representative ICC images of monocultured PDPN-expressing SSC progenies stained *in vitro* with type IV collagen (*A*) and laminin isoforms (*B*). *C–F*, basement membrane ECM deposition at the periluminal space in the xenovascular model. *C* and *E*, representative ICC images of the xenovascular model cocultured with HUVECs and PDPN-expressing SSC progenies stained *in vitro* with type IV collagen (*C*) and laminin isoforms (E). *D* and *F*, quantitative area analysis of deposited type IV collagen (*D*) and laminin isoforms (*F*) in the xenovascular model. $^{**}p < 0.01$. $^{****}p < 0.0001$. Statistical analysis was performed using the Student's *t* test (n = 5 per group). The error bars represent SEMs. All scale bar indicates 50 μm. ECMs, extracellular matrices; HUVECs, human umbilical vein endothelial cells; ICC: immunocytochemistry, PDPN, podoplanin; SSC, skeletal stem cell.

Jagged2 (JAG2), delta-like 1 (DLL1), and delta-like 4 (DLL4) (47). We stimulated SSC progenies with recombinant Notch ligand-immunoglobulin G (IgG) Fc fusion proteins (JAG1-Fc, JAG2-Fc, DLL1-Fc, and DLL4-Fc) and evaluated the expression of vascular basement membrane ECM-related genes (Fig. 9, *G–L*). *Hes1* is a gene that is upregulated upon Notch signal activation. All Notch ligand-Fc proteins significantly upregulated *Hes1* expression (Fig. 9*G*). In collagenous ECM-related genes, *Col4a1* expression was upregulated in the stimulation with JAG1-Fc and JAG2-Fc (Fig. 9*H*). *Col4a2* expression was elevated upon the stimulation with JAG1-Fc, DLL1-Fc, and DLL4-Fc (Fig. 9*I*). Considering that the upregulation of *Col4a1* and *Col4a2* expression was significantly suppressed with a Notch pathway inhibitor in the SSC progenies cocultured with HUVECs (Fig. 9, *B* and *C*), the *Col4a1* and *Col4a2* expressions were specifically and synergistically upregulated *via* the stimuli of Notch ligands. In the noncollagenous ECM-related genes, JAG2-Fc exhibited a weak tendency of *Lama5* upregulation; however, it was not statistically significant (Fig. 9*J*). The expression of *Nid1* was not significantly altered with any recombinant Notch ligand stimulation (Fig. 9*K*). Given a weak inhibitory effect of Notch pathway inhibitor on *Lama5* and *Nid1* expression (Fig. 9, *D* and *E*), the upregulation of *Lama5* and *Nid1* may be attributed to other stimulation(s) except Notch pathway activation. *Nid2* expression was significantly suppressed in the SSC progenies cocultured with HUVECs (Fig. 8*H*) and not responded to a Notch pathway inhibitor (Fig. 9*F*). In contrast, recombinant Notch ligand stimulations revealed that JAG1-Fc and DLL4-Fc increased in *Nid2* expression level (Fig. 9*L*). These observations suggest that *Nid2* expression is strongly suppressed *via* signal(s) other than the Notch pathway on the SSC-progeny–HUVEC interaction. In the cell–cell interaction of the PDPN-expressing SSC progenies and HUVECs, the Notch pathway is

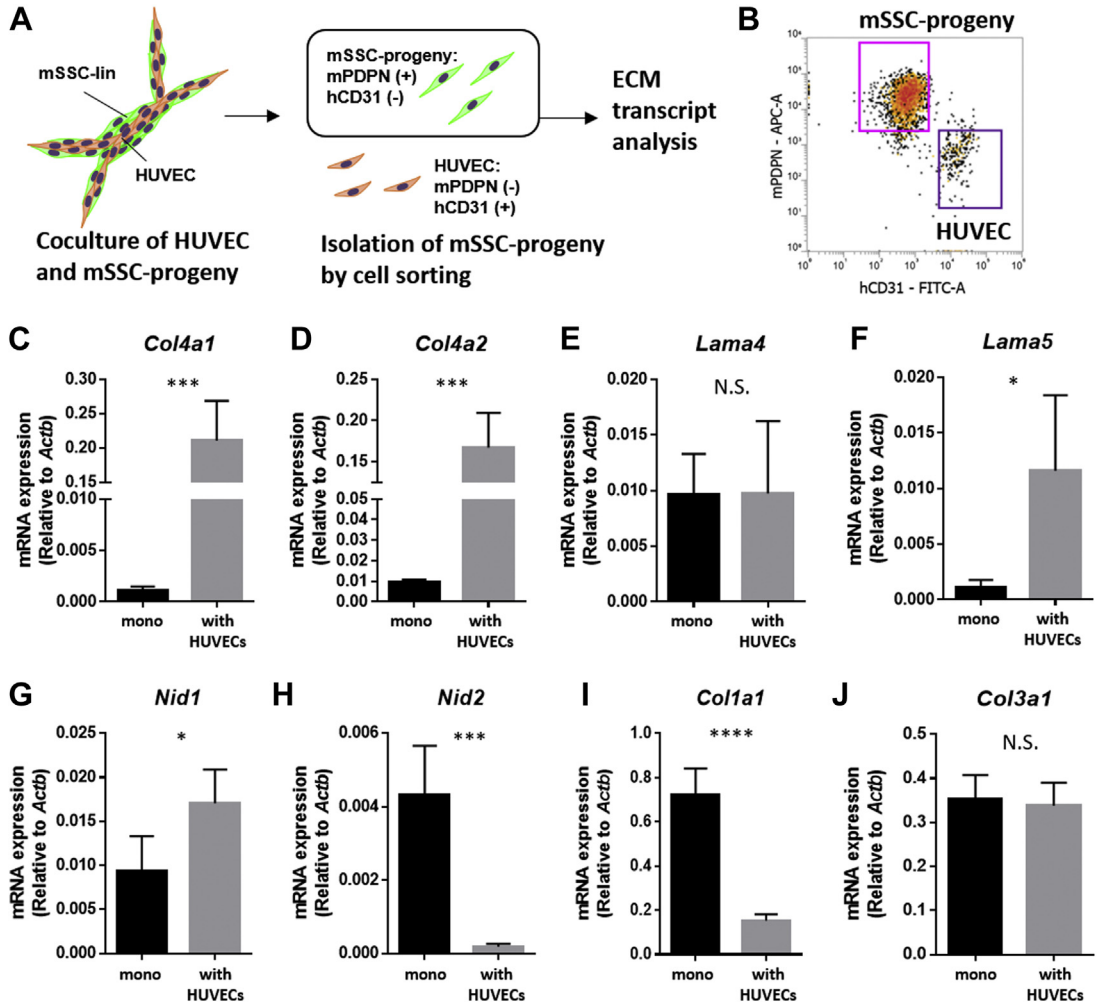

Figure 8. Cell–cell interaction with HUVECs commits PDPN-expressing SSC progenies into a pericyte-phenotype with basement membrane–ECM dominant state. *A*, strategy for isolating cocultured PDPN-expressing SSC progenies in the xenovascular model. *B*, representative flow cytometric scattergram detecting HUVECs and PDPN-expressing SSC progenies *via* the staining of human CD31 and mouse PDPN. Distinctively separated mouse PDPN-expressing SSC progenies were isolated using the cell sorter. *C–H*, RT-qPCR evaluating the expression of the genes encoding proteins present in vascular basement membrane-related ECMs. Collagenous basement membrane ECMs genes: type IV collagen alpha-chains *Col4a1* (*C*) and *Col4a2* (*D*). Non-collagenous basement membrane ECMs are as follows: laminin alpha-chains *lama4* (*E*) and *lama5* (*F*), and nidogen isoforms *Nid1* (*G*) and *Nid2* (H). *I* and *J*, RT-qPCR evaluating the expression of genes encoding the proteins present in nonvascular basement membrane ECMs, such as fibrillar type I and type III collagen *Col1a1* (I) and *Col3a1* (J). *$p < 0.01$. ***$p < 0.01$. ****$p < 0.0001$. N.S. indicates nonsignificance differences. Statistical analysis was performed by the Student's *t* test (n = 5 per group). The error bars represent SEMs. ECM, extracellular matrix; HUVECs, human umbilical vein endothelial cells; PDPN, podoplanin; RT-qPCR, reverse transcribed-quantitative PCR; SSC, skeletal stem cell.

one of the key regulatory mechanisms to commit the PDPN-expressing SSC progenies into a dominant state with basement membrane-related collagenous ECMs.

Discussion

Bone marrow PDPN-expressing stromal cells generate megakaryopoietic and erythropoietic microenvironments in the perivascular space of the bone marrow in adult mice (28, 29). However, their contribution to marrow development and homeostasis has been unclear. In this study, we observed that PDPN-positive periosteal cells infiltrated the cartilaginous anlage of the postnatal epiphysis and populated on the primitive SOC vasculature (Fig. 10*A*). In addition, we revealed that PDPN-expressing stromal cells were subpopulation of the SSC lineage. Based on the findings obtained using the *in vitro* xenovascular model, we propose that PDPN-expressing stromal cells maintain vascular integrity *via* the release of angiogenic factors and vascular basement membrane ECM-related molecules (Fig. 10*B*). In addition, Notch signal activations in the cell–cell interaction with endothelial cells commit the PDPN-expressing stromal cells into a dominant state with basement membrane-related ECMs, especially type IV collagens.

PDPN is a mucin-type transmembrane protein that binds to C-type lectin-like receptor-2 (CLEC-2, also known as CLEC1B) expressed on platelets and megakaryocytes (48–50). In non-bone marrow tissues, PDPN is expressed by multiple cell types (51), such as type I alveolar epithelial cells (52) and lymphatic endothelial cells (53). The interaction between PDPN on type I alveolar epithelial cells and CLEC-2 on platelets regulates neonatal lung development (54). The

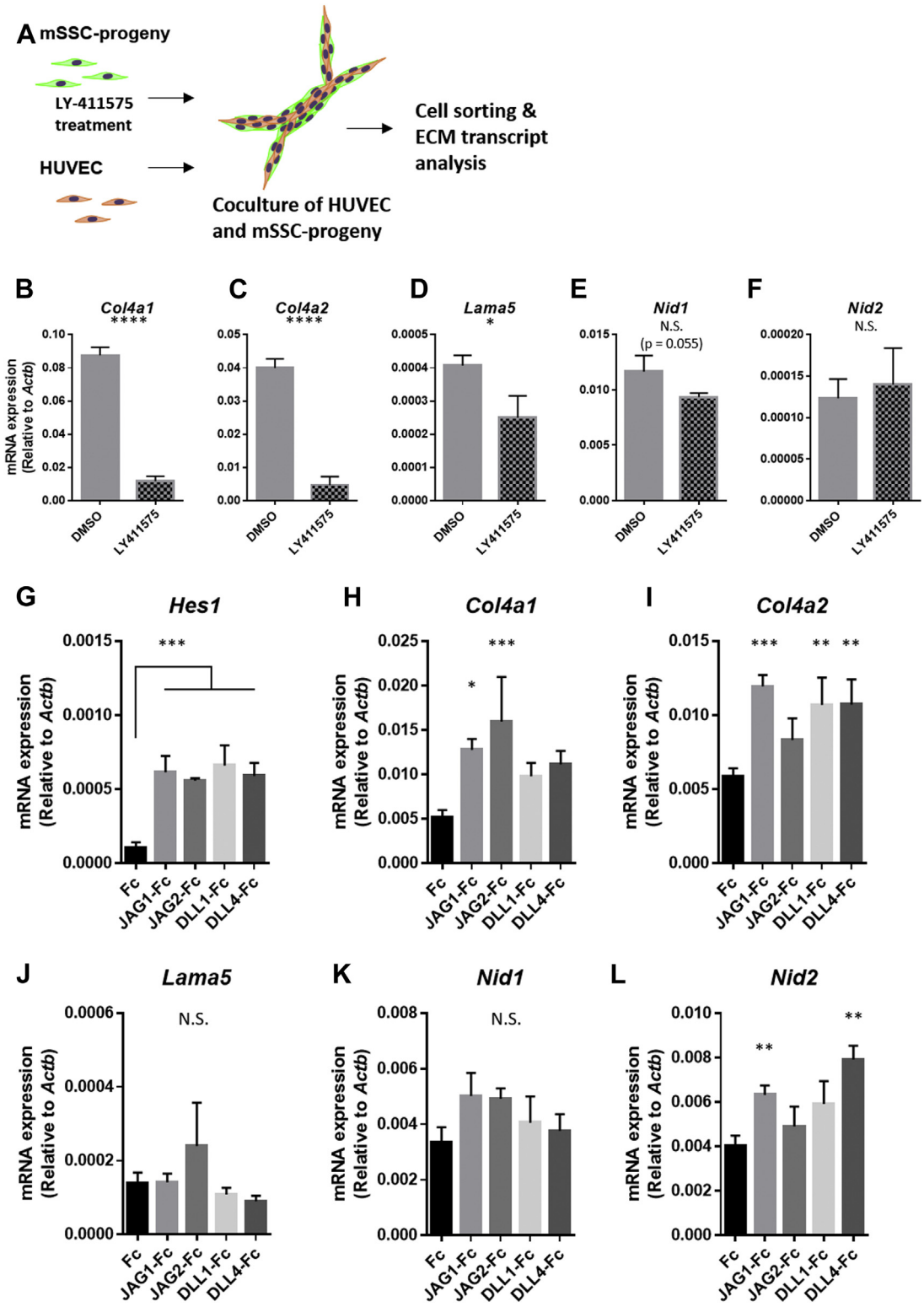

Figure 9. Notch pathway regulates gene expression of basement membrane-related collagenous ECMs in PDPN-expressing SSC progenies. *A*, strategy for experiments involving the xenovascular model and LY-411575, a Notch pathway inhibitor. Prior to their coculture with HUVECs, PDPN-expressing SSC progenies were pretreated with LY-411575 *in vitro*. Isolated PDPN-expressing SSC progenies were subjected to ECM transcript analysis. *B–F*, LY-411575 suppresses the basement membrane ECM upregulation of PDPN-expressing SSC progenies during cell–cell interactions with HUVECs. In this experiment, we targeted the ECM genes *Col4a1* (*B*), *Col4a2* (*C*), *Lama5* (*D*), *Nid1* (*E*), and *Nid2* (*F*), which were altered during coculture with HUVECs. *G–L*, RT-qPCR evaluating the expression of the genes encoding proteins present in vascular basement membrane-related ECMs under Notch stimulation with recombinant Notch ligands. (*G*) All recombinant Notch ligands upregulated *Hes1* expression. The expression levels of collagenous or noncollagenous basement membrane ECMs genes: type IV collagen alpha-chains *Col4a1* (*H*) and *Col4a2* (*I*) laminin alpha-chains *lama5* (*J*), and nidogen isoforms *Nid1* (*K*) and *Nid2* (L). *$p < 0.01$. **$p < 0.01$. ***$p < 0.01$. ****$p < 0.0001$. N.S. indicates nonsignificance differences. For panel *B–F*, comparison between two groups was performed by the Student's *t* test (n = 5 per group). For panel *G–L*, multi-group comparison was performed by one-way ANOVA and Dunnett's *t* test (n = 5 per group, control group: Fc). The error bars represent SEMs. ECM, extracellular matrix; HUVECs, human umbilical vein endothelial cells PDPN, podoplanin; RT-qPCR, reverse transcribed-quantitative PCR; SSC, skeletal stem cell.

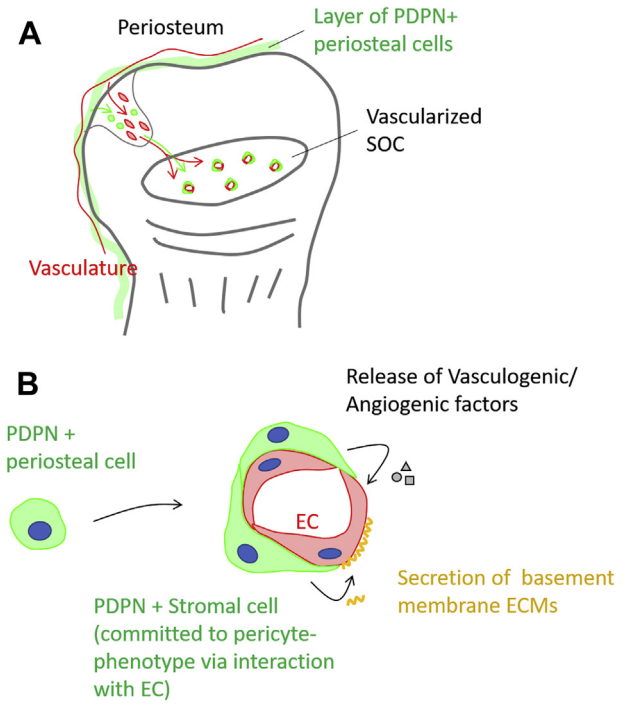

Figure 10. Graphical model depicting the proposed role of PDPN-expressing stromal cells in epiphyseal marrow development and homeostasis. *A*, marrow PDPN-expressing stromal cells originate from periosteal cellular components. PDPN-positive periosteal cells invade into the avascular cartilaginous anlage of the postnatal epiphysis and populate the SOC as PDPN-expressing stromal cells. Marrow PDPN-expressing stromal cells behave in a manner similar to the pericytes of the primitive SOC vasculature. *B*, Marrow PDPN-expressing stromal cells are the subpopulation of the SSC lineage. Based on the results obtained using the xenovascular model in *in vitro* experiments, we propose that marrow PDPN-expressing stromal cells maintain the vascular integrity by secreting angiogenic factors and vascular basement membrane ECMs. In response to the Notch-mediated interaction with endothelial cells, marrow PDPN-expressing stromal cells commit to a dominant state with basement membrane-related ECMs, especially type IV collagens. ECMs, extracellular matrices ; PDPN, podoplanin; SOC, secondary ossification center; SSC, skeletal stem cell;.

interaction of PDPN on lymphatic endothelial cells and CLEC-2 on platelets promotes lymphatic vessel development in the embryos (55, 56). The PDPN–CLEC-2 axis is a key determinant of vascular integrity that maintains vascularized tissue homeostasis and development. In the lymph node, fibroblastic reticular cells express PDPN and maintain lymph node homeostasis by regulating the integrity of high endothelial venules(57, 58). During lymph node hemorrhage (*e.g.*, increased lymphocyte trafficking such as chronic inflammation), fibroblastic reticular cell PDPN interacts with CLEC-2 on extravasated platelets. The platelets activated *via* the PDPN–CLEC-2 axis locally release sphingosine-1-phosphate in the perivenular space, causing increased high endothelial venule integrity (57). Given that PDPN molecule does not directly affect vascular integrity (Fig. S6), we consider that bone marrow PDPN-expressing stromal cells contribute to nascent marrow homeostasis by consolidating vascular integrity such as the PDPN–CLEC-2 axis in the lymph node.

ECM molecules play an important role in the formation of the vasculature and maintenance of its integrity. In the vascular system, the ECM forms two types of structures, that is, the interstitial matrix and the basement membrane (44). The basement membrane is a sheet-like structure composed of type IV collagen, laminins (laminin-411 and laminin-511), nidogens, and perlecan, which represents a physiological barrier to the movement of intra/extravascular soluble molecules and migrating cells (45, 59). In addition, the basement membrane provides a scaffold that supports vascular lumen formation and the interaction between the endothelium and pericytes (60). The use of *in vitro* PDPN-expressing SSC progenies in our xenovascular model suggests that PDPN-expressing stromal cells prime the perivascular environment *via* the secretion of basement membrane ECM molecules (Fig. 7, *C–F*). Further, we observed that PDPN-expressing SSC progenies switched their ECM expression pattern, which causes the dominance of basement membrane components (Fig. 8). Endothelial cells express Notch ligands which activate the Notch pathway in pericytes or perivascular cells *via* cell–cell interactions (61–65). Knockout of Notch pathway intermediaries causes vascular defects or pericyte dysfunction (66–70). In the PDPN-expressing stromal cells, Notch ligands markedly upregulate basement membrane-related collagenous ECMs, for example, *COL4a1* and *Col4a2* (Fig. 9). These evidences indicate the important role played by Notch signaling in vascular development. We hypothesize that bone marrow PDPN-expressing stromal cells switch their cellular phenotype to the dominance of basement membrane-related collagenous ECMs *via* Notch-mediated interaction with the endothelium, and this process promotes marrow vascularization.

In this study, we have shown the vascular regulatory functions of epiphyseal marrow PDPN-expressing stromal cells using the *in vitro* xenovascular model. However, this study has a few limitations. To further demonstrate their role in bone marrow physiology including disease pathophysiology, an *in vivo* cell-fate reporter, conditional knockout, or depletion model that specifically targets the marrow PDPN-expressing stromal cells must be established. These *in vivo* models would demonstrate the detailed mechanism by which PDPN-expressing stromal cells regulate bone marrow development and homeostasis, or endochondral ossification process. Furthermore, it must be examined whether the marrow PDPN-expressing stromal cells are involved in bone marrow development during embryogenesis (especially POC-associated marrow development). These questions need to be addressed in future studies.

Our study offers a new perspective in understating how stromal cells regulate nascent bone marrow development and homeostasis. This study can be used as a basis for further studies to comprehensively examine the contribution of stromal cells to the developmental physiology of the bone marrow. This would provide insights into the mechanism of the bone and bone marrow development

Experimental procedures

Mice

C57BL/6NcrSlc mice were purchased from CLEA Japan, Inc. They were bred and maintained under standard

conditions [a 12 h light/dark cycle with stable temperature (25 °C) and humidity (60%)]; the mice that were 7 to 21 postnatal days old were selected for the experiments. This study was approved by the animal care and use committee at the Nagoya University Faculty of Medicine(D210596-003).

Flow cytometry

Femurs were harvested from mice at P21. To obtain epiphyseal marrow stromal cells, dissected epiphyses were gently smashed using a mortar and further cut to small pieces. After a few washes with ice-cold PBS containing 10% fetal bovine serum (FBS, Sigma-Aldrich), the epiphyseal pieces were digested with 0.2% (w/v) collagenase (Wako) for 2 h at 37 °C and agitated at 100 rpm. After collagenase digestion, the epiphyseal pieces were further crushed in a mortar with ice-cold PBS containing 10% FBS. Harvested cells were passed through a 40-μm cell strainer (Corning). The cell suspension was centrifuged at 280*g* for 5 min at 4 °C. The cell pellet was hemolyzed with sterilized ultrapure water for 6 s and washed with ice-cold PBS containing 10% FBS.

To obtain diaphyseal marrow stromal cells, the marrow was flushed from the dissected diaphysis using a 21-gauge needle (Terumo). The flushed diaphyseal marrow was suspended in ice-cold PBS containing 10% FBS and passed through a 40-μm cell strainer. After centrifugation, the cell pellet was resuspended and hemolyzed using the ACK buffer (155 mM NH_4Cl, 10 mM $KHCO_3$, 0.1 mM EDTA). The hemolyzed cells were probed with antibodies against hematopoietic lineage markers (CD4, CD8, B220, TER-119, Ly-6G, CD11b, F4/80, and CD71). Cells of the hematopoietic lineage were depleted using sheep anti-rat IgG polyclonal antibody–conjugated magnetic beads (Dynabeads, Thermo Fisher Scientific). Cells that were not of hematopoietic lineage were harvested and washed with ice-cold PBS containing 10% FBS. For enrichment of PDPN-positive cells, epiphyseal or diaphyseal stromal cells were probed using the anti-PDPN APC conjugate (Clone: 8.1.1, Biolegend) and isolated as APC-positive fraction using anti-APC Microbeads (Miltenyi Biotec) on an LS column (Miltenyi Biotec). The depletion antibodies used in the study are listed in Table S1.

Harvested cells were probed with fluorescence-conjugated antibodies or their isotype controls. Flow cytometry was performed using a three-laser Attune N × T (E × .405/488/637 nm, Thermo Fisher Scientific). Cell sorting was performed using a four-laser FACS Aria II (E × .355/407/488/633 nm, BD Bioscience). The fluorescence-conjugated antibodies used in this study are listed in Table S1.

Immunohistochemistry

Femurs were fixed with 4% paraformaldehyde (PFA, Wako) for 24 h and subsequently decalcified for 16 h using K-CX (FALMA). After washing with diluted water, bone pieces were incubated in 30% sucrose (Wako) for cryoprotection. Treated tissues were embedded in Tissue-Tek O.C.T. Compound (Tissue-Tek) at −80 °C. Frozen sections were sectioned to generate 10-μm-thick sections and blocked with PBS–containing 3% bovine serum albumin (Sigma-Aldrich) and 2% goat serum (Sigma-Aldrich). Sections were probed overnight with primary antibodies against PDPN, VE-cadherin, NG2, and αSMA—diluted with the blocking reagent—at 4 °C. Then, the sections were probed with secondary antibody conjugates, including anti-Syrian hamster IgG Alexa 488 conjugate (for PDPN, A21110, Thermo Fisher Scientific, 1:1000 diluted) and anti-rabbit IgG Alexa 568 conjugate (for VE-cadherin, PDGFRβ, and NG2, A11034, Thermo Fisher Scientific, 1:2000 diluted), and anti-mouse IgG Alexa 568 conjugate (for αSMA, A11004, Thermo Fisher Scientific, 1:2000 diluted) for 1.5 h at 25 °C. The sections were mounted with VECTASHIELD Antifade Mounting Medium containing DAPI (Vector Laboratories) and observed under an upright fluorescence microscope (AX80, Olympus). The primary antibodies used in the study are listed in Table S1.

Immunocytochemistry

Cells were seeded onto 15-mm Fisherbrand Coverglass for Growth Cover Glasses (Thermo Fischer Scientific) and cultured in 12-well culture plates at 37 °C, 5% CO_2. HUVECs were passaged 4 to 8 times, whereas primary SSCs were passaged <3 times. The cells were fixed with 4% PFA. To achieve permeabilization, cells were incubated with 0.1% Triton X-100 (Wako) prepared in PBS for 10 min. After washing with PBS, the cells were blocked with PBS containing 3% bovine serum albumin and 2% goat serum for 1 h at 25 °C. Cells were probed overnight with primary antibodies against PDPN, VE-cadherin, NG2, αSMA, COL4, and laminins at 4 °C. Then cells were probed with secondary antibody conjugates, including anti-Syrian hamster IgG Alexa 488 conjugate (for PDPN, A21110, Thermo Fisher Scientific, 1:1000 diluted) and anti-rabbit IgG Alexa 568 conjugate (for VE-cadherin, PDGFRβ, NG2, COL4, and laminins, A11034, Thermo Fisher Scientific, 1:2000 diluted), and anti-mouse IgG Alexa 568 conjugate (for αSMA, A11004, Thermo Fisher Scientific, 1:2000 diluted) for 1.5 h at 25 °C. Cells were mounted using VECTASHIELD Antifade Mounting Medium containing DAPI (Vector Laboratories) and observed under an inverted fluorescence microscope (IX73, Olympus). Acquired images were quantitatively analyzed using Image J 1.46r (http://rsb.info.nih.gov/ij/).

Cell culture

HUVECs (TaKaRa Bio) were cultured using EGM2 (TaKaRa Bio) and penicillin/streptomycin/amphotericin B (Wako). Isolated mouse primary SSCs were cultured using the mouse MesenCult Expansion Kit with L-glutamine (Wako) and penicillin/streptomycin/amphotericin B (Wako).

Colony formation assay

Isolated cells were seeded onto a 12-well culture plate (1000 cells/well, Thermo Fisher Scientific) and cultured using the Complete MesenCult expansion medium (Stem Cell Technologies) for 7 days. Cells were stained with Giemsa staining solution (Muto pure chemicals).

In vitro *mesenchymal tri-lineage differentiation*

For osteogenic differentiation, cells were seeded into a 24-well plate (4×10^5 cells/cm^2) and cultured using the

Complete MesenCult expansion medium. After 24 h, the culture medium was replaced with the Complete mouse MesenCult Osteogenic Medium (Stem Cell Technologies) containing L-glutamine (Wako) and penicillin/streptomycin/amphotericin B (Wako), and the cells were cultured for 12 days. Osteoblastic differentiation was investigated by evaluating calcium deposition *via* Von Kossa staining. Briefly, cells were fixed with 4% PFA and washed with PBS. After rinsing the cells with distilled water, the deposited calcium was stained using a Calcium Stain Kit (ScyTek laboratories); cells were subsequently counterstained with the Fast Red solution.

To achieve adipogenic differentiation, cells were seeded in a 24-well plate (1×10^5 cells/cm^2) and maintained using the Complete MesenCult expansion medium. After 24 h, the culture medium was replaced with the Complete mouse MesenCult Adipogenic Differentiation Medium (Stem Cell Technologies) containing L-glutamine (Wako) and penicillin/streptomycin/amphotericin B (Wako), and cells were cultured for 12 days. Adipogenic differentiation was evaluated by staining adipocytes with Oil Red O (Wako). A working solution of Oil Red O was prepared by mixing Oil Red O stock solution [0.15 g Oil Red O (Wako) in 100% isopropanol (Wako)] and distilled water at a dilution of 6:4. It was filtered after 20 min. Cells were fixed with 4% PFA, washed with PBS, and incubated with 60% isopropanol for 1 min. Then, cells were incubated for 20 min with a working solution of Oil red O at room temperature, rinsed with 60% isopropanol, and washed twice with PBS.

To achieve chondrogenic differentiation, cells were seeded in a 24-well plate (4×10^5 cells/cm^2) and cultured using the Complete MesenCult expansion medium. After 24 h, the culture medium was replaced with the Complete mouse MesenCult-ACF Chondrogenic Differentiation Medium (Stem Cell Technologies) and penicillin/streptomycin/amphotericin B (Wako), and the cells were cultured for 12 days. Chondrogenic differentiation was evaluated by staining chondrocyte-associated mucopolysaccharides with Alcian Blue. Cells were fixed with 4% PFA, washed with PBS, and treated with 3% acetic acid. Then, cells were incubated with an Alcian Blue (pH of 2.5; Muto Pure Chemicals) for 30 min at room temperature and washed with 3% acetic acid. After rinsing with distilled water, the cells were counterstained with the Fast Red solution for 5 min and washed twice with distilled water.

RNA extraction and reverse transcribed-quantitative PCR

Total RNA was extracted by using the ReliaPrep RNA Cell Miniprep System (Promega). First strand complementary DNA (cDNA) was synthesized using the PrimeScript II first strand cDNA Synthesis Kit (TaKaRa Bio), according to the manufacturer's instructions. Multiplex qPCR was performed using the TaqMan Gene expression Master Mix (Thermo Fisher Scientific), PrimeTime qPCR Assay (Integrated DNA Technology), and Thermal Cycler Dice Real Time System (TaKaRa Bio). The cycling conditions were as follows: 95 °C for 10 min and 40 cycles of denaturation at 95 °C for 15 s and annealing/extension at 60 °C for 1 min. Fluorescence intensity was measured at every annealing/extension step. The qPCR probes used in this study are listed in Table S2.

HUVEC capillary formation and xenovascular model

HUVECs (0.53×10^5/cm^2) and/or *in vitro* SSC progenies (0.39×10^5/cm^2) were seeded onto a cell culture plate or coverglass 8-well chamber (Iwaki) coated with the Corning Matrigel Growth Factor Reduced Basement Membrane Matrix (Corning) and cultured with Complete EGM2 supplemented with 2% Matrigel and 10 ng/ml VEGF-A (Miltenyi Biotech). HUVEC lumen integrity was analyzed using the Angiogenesis Analyzer for ImageJ tool (http://image.bio.methods.free.fr/ImageJ/?Angiogenesis-Analyzer-for-ImageJ&lang=en). To evaluate the vascular lumen integrity, we determined several parameters, that is, the number of junctions, the number of segments (segments are elements delimited by two junctions), the number of meshes (meshes are areas enclosed by segments), and the total mesh area.

For blockage of VEGF-A–VEGFR2 interaction, neutralizing antibodies against mouse VEGF-A (AF-493-NA; R&D Systems) or human VEGFR2 (MAB3572, R&D Systems) were added into HUVEC tube formation assay.

For Notch pathway inhibition, *in vitro* SSC progenies were treated with 1 μM LY-411575 (Sigma-Aldrich) for 24 h and reseeded into the xenovascular model with HUVECs. To achieve the dissociation of *in vitro* SSC progenies in the xenovascular model, xenovascular lumens were gently washed with PBS and digested with 1 mg/ml of collagenase/dispase (Sigma-Aldrich) for 10 min at 37 °C. After enzymatic digestion, cells were resuspended in PBS and gently mixed *via* the pipetting action 10 times, followed by centrifugation at 300*g* for 5 min. Harvested cells were resuspended in PBS containing 10% FBS and probed with anti-mouse PDPN-APC conjugate and anti-human CD31-FITC conjugate. Cell sorting was performed using FACS Aria II (BD Bioscience).

HUVEC proliferation assay

HUVECs were seeded onto a 96-well plate (6.25×10^3/cm^2) and cultured in complete EGM-2 medium. After preculture for 24 h, the culture medium was replaced with the complete EGM-2, Non-CM, and SSC progeny–conditioned medium. Cell proliferation was assessed using the WST-8 assay based Cell Counting Kit-8 (DOJINDO LABORATORIES).

HUVEC scratch assay

HUVECs were seeded onto a 24-well plate (0.52×10^4/cm^2) and cultured with the complete EGM-2 medium until complete confluency was achieved. HUVEC monolayers were starved of EGM-2 for 3 h and scratched using a sterilized 1 ml micropipette tip. The scratched HUVEC monolayers were cultured using a Non-CM or SSC progeny–conditioned medium for 24 h. At 0 h and 24 h, microscopy-based images were obtained using inverted optical microscopy (CKX53, Olympus), and the covered area was analyzed using Image J 1.46r.

Protein array

Angiogenic regulators profiled in the conditioned medium were analyzed using the Proteome Profiler Mouse

Angiogenesis Array Kit (ARY015; R&D Systems). We loaded the conditioned medium (1 ml) onto the array membrane, as per the manufacturer's instructions. We used ECL Prime (GE Healthcare) as a horseradish peroxidase substrate and detected chemiluminescence signals using the Light Capture II system (Atto Corporation). Quantification analysis was performed using Image J 1.46r.

Preparation of recombinant mouse PDPN-human IgG Fc2 fusion protein (mPDPN-hFc2)

A cDNA fragment of mouse PDPN extracellular domain was obtained from a mouse bone marrow cDNA library. Mouse bone marrow total RNA was extracted using ReliaPrep RNA Cel l Miniprep System (Promega). After total RNA extraction, first-strand cDNA was prepared using PrimeScript RT Master Mix II (TaKaRa Bio). A coding sequence of mouse PDPN extracellular domain was amplified by PCR using KOD FX (Toyobo) and primer set (Fw: 5′-GGGGCCATGGGGGACTATAGGCGTGA ATGAAGATG-3′, Rv: 5′-GGGGAGATCTCAGGGTGACTA CTGGCAAGC-3′, underlines in Fw and Rv indicate *Not*I and *Bgl*II sites, respectively). The PCR amplicon was digested with *Not*I and *Bgl*II and inserted into pFUSE-hIgG1-Fc2 (InvivoGen) with Ligation high ver2.0 (Toyobo). HEK293 cells were grown at 37 °C under 5% CO2 in Dulbecco's modified Eagle's medium (DMEM) (Wako) supplemented with 10% FBS (Sigma-Aldrich) and penicillin/streptomycin/amphotericin B (Wako). mPDPN-hFc2 or hFc2 expression vector was transiently transfected into HEK293 cells by electroporation using NEPA21 (Nepa gene). In the following 4 days cultured with Opti-MEM (Invitrogen), culture medium was harvested and removed debris by centrifugation at 3000*g* for 10 min at 4 °C. Recombinant proteins were purified by Hitrap Protein G column (GE Healthcare) using Perista pump (Atto). The proteins were dialyzed against distilled water by Spectra/Por biotech membrane 3.1 (Repligen) and lyophilized by freeze dryer (FDU-2110, EYELA) connected to a drying chamber (DRC-1100, EYELA). The lyophilized recombinant proteins were reconstituted with PBS. Protein concentration was determined using Bio-Rad DC Protein Assay Kit (BioRad Laboratories).

Notch stimulation with immobilized recombinant ligands

Recombinant Notch ligand-IgG Fc fusion proteins (JAG1-Fc, JAG2-Fc, DLL1-Fc, and DLL4-Fc) or recombinant human IgG1 Fc (Fc) were obtained from R&D Systems. Twenty four-well culture plates were coated with 20 nM recombinant Notch ligands or Fc for 24 h at 4 °C. Cells suspended with Complete MesenCult expansion medium were seeded at $2.0 \times 10^4/cm^2$ into the recombinant protein-coated culture plate. After 24 h stimulation, the cells were harvested and subjected to following experiments.

Statistical analysis

Quantitative data are depicted as mean ± SD values of the mean or mean ± standard error values of the mean. Representative data from at least three independent experiments are shown for immunohistochemistry and ICC images. Two-group comparisons were made using the unpaired Student's *t* test. Multi-group comparisons were made using one-way ANOVA and Tukey' multiple comparison test or two-way ANOVA and Sidak's multiple comparison test. Statistical analyses were performed using GraphPad Prism 5 (GraphPad Software).

Data availability

All data supporting the findings of this study are available from the corresponding authors upon reasonable request.

Supporting information—This article contains supporting information.

Author contributions—S. T., N. T., A. K., A. T., J. U., M. H., K. S.-I., and T. M. methodology; S. T., M. M., Y. K., W. F., K. O., K. I., M. H., investigation; S. T., N. S., S. O., A. S., and T. K. formal analysis; S.T. writing–original draft; S. T., N. T., A. K., A. T., K. I., J. U., M. H., K. S.-I., T. M., T. Kojima, and F. H. supervision; S. T., T. Kojima, and F. H. conceptualization; S. T., M. M., Y. K., W. F., K. O., N. S., N. T., S. O., A. S., T. K., A. K., A. T., K. I., J. U., M. H., K. S.-I., T. M., T. Kojima, and F. H. writing–review and editing; S. T., M. M., Y. K., W. F., K. O., N. S., N. T., S. O., A. S., T. K., data curation; S. T., A. K., T. M., T. Kojima, and F. H. funding acquisition; S. T. validation; S. T. visualization; S. T. project administration; K. S.-I. resources.

Funding and additional information—This study was supported by grants-in-aid provided by the Japanese Ministry of Education, Culture, Sports, Science, and Technology (Grant No. 17H05073: S. T and Grant No. 19K08853: A. K), the National Center for Geriatrics and Gerontology (NCGG, the Research Funding for Longevity Sciences, Grant No. 30-11: A. K), the Takeda Science Foundation (S. T), and the SENSHIN Medical Research Foundation (S. T). F. H. received research funding from Daiichi Sankyo, Chugai Pharmaceutical Co, Ltd, Astellas Pharma Inc, and MSD.

Conflict of interest—The authors declare that they have no conflicts of interest with the contents of this article.

Abbreviations—The abbreviations used are: αSMA, alpha smooth muscle actin; BCSPs, bone cartilage stroma progenitors; BM-SSCs, bone marrow SSCs; cDNA, complementary DNA; CLEC-2, C-type lectin-like receptor-2; DLL1, delta-like 1; DLL1, delta-like 4; ECM, extracellular matrix; EGM2, endothelial cell growing medium; FBS, fetal bovine serum; HUVECs, human umbilical vein endothelial cells; ICC, immunocytochemistry; IgG, immunoglobulin G; JAG1, Jagged1; JAG2, Jagged2; NG2, neuron-glial antigen 2; Non-CM, nonconditioned medium; PDGFRβ, platelet-derived growth factor receptor β; PDPN, podoplanin; PFA, paraformaldehyde; POC, primary ossification center; Sca-1, stem cell antigen-1; SOC, secondary ossification center; SSC, skeletal stem cell; VE, vascular endothelial; VEGF-A, vascular endothelial growth factor-A; VEGFR2, vascular endothelial growth factor receptor 2.

References

1. Hanoun, M., and Frenette, P. S. (2013) This niche is a maze; an amazing niche. *Cell Stem Cell* **12**, 391–392
2. Morrison, S. J., and Scadden, D. T. (2014) The bone marrow niche for haematopoietic stem cells. *Nature* **505**, 327–334

3. Kronenberg, H. M. (2003) Developmental regulation of the growth plate. *Nature* **423**, 332–336
4. Karsenty, G., and Wagner, E. F. (2002) Reaching a genetic and molecular understanding of skeletal development. *Dev. Cell* **2**, 389–406
5. Maes, C., Kobayashi, T., Selig, M. K., Torrekens, S., Roth, S. I., Mackem, S., Carmeliet, G., and Kronenberg, H. M. (2010) Osteoblast precursors, but not mature osteoblasts, move into developing and fractured bones along with invading blood vessels. *Dev. Cell* **19**, 329–344
6. Ambrosi, T. H., Longaker, M. T., and Chan, C. K. F. (2019) A revised perspective of skeletal stem cell biology. *Front. Cell Dev. Biol.* **7**, 189
7. Bianco, P., and Robey, P. G. (2015) Skeletal stem cells. *Development* **142**, 1023–1027
8. Tournaire, G., Stegen, S., Giacomini, G., Stockmans, I., Moermans, K., Carmeliet, G., and van Gastel, N. (2020) Nestin-GFP transgene labels skeletal progenitors in the periosteum. *Bone* **133**, 115259
9. Ortinau, L. C., Wang, H., Lei, K., Deveza, L., Jeong, Y., Hara, Y., Grafe, I., Rosenfeld, S. B., Lee, D., Lee, B., Scadden, D. T., and Park, D. (2019) Identification of functionally distinct Mx1+alphaSMA+ periosteal skeletal stem cells. *Cell Stem Cell* **25**, 784–796.e785
10. Duchamp de Lageneste, O., Julien, A., Abou-Khalil, R., Frangi, G., Carvalho, C., Cagnard, N., Cordier, C., Conway, S. J., and Colnot, C. (2018) Periosteum contains skeletal stem cells with high bone regenerative potential controlled by Periostin. *Nat. Commun.* **9**, 773
11. Deveza, L., Ortinau, L., Lei, K., and Park, D. (2018) Comparative analysis of gene expression identifies distinct molecular signatures of bone marrow- and periosteal-skeletal stem/progenitor cells. *PLoS One* **13**, e0190909
12. Sugiyama, T., Kohara, H., Noda, M., and Nagasawa, T. (2006) Maintenance of the hematopoietic stem cell pool by CXCL12-CXCR4 chemokine signaling in bone marrow stromal cell niches. *Immunity* **25**, 977–988
13. Omatsu, Y., Sugiyama, T., Kohara, H., Kondoh, G., Fujii, N., Kohno, K., and Nagasawa, T. (2010) The essential functions of adipo-osteogenic progenitors as the hematopoietic stem and progenitor cell niche. *Immunity* **33**, 387–399
14. Omatsu, Y., Seike, M., Sugiyama, T., Kume, T., and Nagasawa, T. (2014) Foxc1 is a critical regulator of haematopoietic stem/progenitor cell niche formation. *Nature* **508**, 536–540
15. Ara, T., Tokoyoda, K., Sugiyama, T., Egawa, T., Kawabata, K., and Nagasawa, T. (2003) Long-term hematopoietic stem cells require stromal cell-derived factor-1 for colonizing bone marrow during ontogeny. *Immunity* **19**, 257–267
16. Zhou, B. O., Yue, R., Murphy, M. M., Peyer, J. G., and Morrison, S. J. (2014) Leptin-receptor-expressing mesenchymal stromal cells represent the main source of bone formed by adult bone marrow. *Cell Stem Cell* **15**, 154–168
17. Yue, R., Zhou, B. O., Shimada, I. S., Zhao, Z., and Morrison, S. J. (2016) Leptin receptor promotes adipogenesis and reduces osteogenesis by regulating mesenchymal stromal cells in adult bone marrow. *Cell Stem Cell* **18**, 782–796
18. Ding, L., Saunders, T. L., Enikolopov, G., and Morrison, S. J. (2012) Endothelial and perivascular cells maintain haematopoietic stem cells. *Nature* **481**, 457–462
19. Park, D., Spencer, J. A., Koh, B. I., Kobayashi, T., Fujisaki, J., Clemens, T. L., Lin, C. P., Kronenberg, H. M., and Scadden, D. T. (2012) Endogenous bone marrow MSCs are dynamic, fate-restricted participants in bone maintenance and regeneration. *Cell Stem Cell* **10**, 259–272
20. Worthley, D. L., Churchill, M., Compton, J. T., Tailor, Y., Rao, M., Si, Y., Levin, D., Schwartz, M. G., Uygur, A., Hayakawa, Y., Gross, S., Renz, B. W., Setlik, W., Martinez, A. N., Chen, X., *et al.* (2015) Gremlin 1 identifies a skeletal stem cell with bone, cartilage, and reticular stromal potential. *Cell* **160**, 269–284
21. Mendez-Ferrer, S., Michurina, T. V., Ferraro, F., Mazloom, A. R., Macarthur, B. D., Lira, S. A., Scadden, D. T., Ma'ayan, A., Enikolopov, G. N., and Frenette, P. S. (2010) Mesenchymal and haematopoietic stem cells form a unique bone marrow niche. *Nature* **466**, 829–834
22. Kunisaki, Y., Bruns, I., Scheiermann, C., Ahmed, J., Pinho, S., Zhang, D., Mizoguchi, T., Wei, Q., Lucas, D., Ito, K., Mar, J. C., Bergman, A., and Frenette, P. S. (2013) Arteriolar niches maintain haematopoietic stem cell quiescence. *Nature* **502**, 637–643
23. Matsushita, Y., Nagata, M., Kozloff, K. M., Welch, J. D., Mizuhashi, K., Tokavanich, N., Hallett, S. A., Link, D. C., Nagasawa, T., Ono, W., and Ono, N. (2020) A Wnt-mediated transformation of the bone marrow stromal cell identity orchestrates skeletal regeneration. *Nat. Commun.* **11**, 332
24. Mizuhashi, K., Ono, W., Matsushita, Y., Sakagami, N., Takahashi, A., Saunders, T. L., Nagasawa, T., Kronenberg, H. M., and Ono, N. (2018) Resting zone of the growth plate houses a unique class of skeletal stem cells. *Nature* **563**, 254–258
25. Chan, C. K., Seo, E. Y., Chen, J. Y., Lo, D., McArdle, A., Sinha, R., Tevlin, R., Seita, J., Vincent-Tompkins, J., Wearda, T., Lu, W. J., Senarath-Yapa, K., Chung, M. T., Marecic, O., Tran, M., *et al.* (2015) Identification and specification of the mouse skeletal stem cell. *Cell* **160**, 285–298
26. Greenbaum, A., Hsu, Y. M., Day, R. B., Schuettpelz, L. G., Christopher, M. J., Borgerding, J. N., Nagasawa, T., and Link, D. C. (2013) CXCL12 in early mesenchymal progenitors is required for haematopoietic stem-cell maintenance. *Nature* **495**, 227–230
27. Asada, N., Kunisaki, Y., Pierce, H., Wang, Z., Fernandez, N. F., Birbrair, A., Ma'ayan, A., and Frenette, P. S. (2017) Differential cytokine contributions of perivascular haematopoietic stem cell niches. *Nat. Cell Biol.* **19**, 214–223
28. Tamura, S., Suzuki-Inoue, K., Tsukiji, N., Shirai, T., Sasaki, T., Osada, M., Satoh, K., and Ozaki, Y. (2016) Podoplanin-positive periarteriolar stromal cells promote megakaryocyte growth and proplatelet formation in mice by CLEC-2. *Blood* **127**, 1701–1710
29. Otake, S., Sasaki, T., Shirai, T., Tsukiji, N., Tamura, S., Takano, K., Ozaki, Y., and Suzuki-Inoue, K. (2021) CLEC-2 stimulates IGF-1 secretion from podoplanin-positive stromal cells and positively regulates erythropoiesis in mice. *J. Thromb. Haemost.* **19**, 1572–1584
30. Baccin, C., Al-Sabah, J., Velten, L., Helbling, P. M., Grunschlager, F., Hernandez-Malmierca, P., Nombela-Arrieta, C., Steinmetz, L. M., Trumpp, A., and Haas, S. (2020) Combined single-cell and spatial transcriptomics reveal the molecular, cellular and spatial bone marrow niche organization. *Nat. Cell Biol.* **22**, 38–48
31. Attwell, D., Mishra, A., Hall, C. N., O'Farrell, F. M., and Dalkara, T. (2016) What is a pericyte? *J. Cereb. Blood Flow Metab.* **36**, 451–455
32. Hartmann, D. A., Underly, R. G., Grant, R. I., Watson, A. N., Lindner, V., and Shih, A. Y. (2015) Pericyte structure and distribution in the cerebral cortex revealed by high-resolution imaging of transgenic mice. *Neurophotonics* **2**, 041402
33. Azar, W. J., Azar, S. H., Higgins, S., Hu, J. F., Hoffman, A. R., Newgreen, D. F., Werther, G. A., and Russo, V. C. (2011) IGFBP-2 enhances VEGF gene promoter activity and consequent promotion of angiogenesis by neuroblastoma cells. *Endocrinology* **152**, 3332–3342
34. Dai, J., Peng, L., Fan, K., Wang, H., Wei, R., Ji, G., Cai, J., Lu, B., Li, B., Zhang, D., Kang, Y., Tan, M., Qian, W., and Guo, Y. (2009) Osteopontin induces angiogenesis through activation of PI3K/AKT and ERK1/2 in endothelial cells. *Oncogene* **28**, 3412–3422
35. Stamatovic, S. M., Keep, R. F., Mostarica-Stojkovic, M., and Andjelkovic, A. V. (2006) CCL2 regulates angiogenesis *via* activation of Ets-1 transcription factor. *J. Immunol.* **177**, 2651–2661
36. Quintero-Fabian, S., Arreola, R., Becerril-Villanueva, E., Torres-Romero, J. C., Arana-Argaez, V., Lara-Riegos, J., Ramirez-Camacho, M. A., and Alvarez-Sanchez, M. E. (2019) Role of matrix metalloproteinases in angiogenesis and cancer. *Front. Oncol.* **9**, 1370
37. Lee, S., Jilani, S. M., Nikolova, G. V., Carpizo, D., and Iruela-Arispe, M. L. (2005) Processing of VEGF-A by matrix metalloproteinases regulates bioavailability and vascular patterning in tumors. *J. Cell Biol.* **169**, 681–691
38. Salcedo, R., and Oppenheim, J. J. (2003) Role of chemokines in angiogenesis: CXCL12/SDF-1 and CXCR4 interaction, a key regulator of endothelial cell responses. *Microcirculation* **10**, 359–370
39. Wu, J., Strawn, T. L., Luo, M., Wang, L., Li, R., Ren, M., Xia, J., Zhang, Z., Ma, W., Luo, T., Lawrence, D. A., and Fay, W. P. (2015) Plasminogen activator inhibitor-1 inhibits angiogenic signaling by uncoupling vascular

endothelial growth factor receptor-2-alphaVbeta3 integrin cross talk. *Arterioscler. Thromb. Vasc. Biol.* **35**, 111–120
40. Isogai, C., Laug, W. E., Shimada, H., Declerck, P. J., Stins, M. F., Durden, D. L., Erdreich-Epstein, A., and DeClerck, Y. A. (2001) Plasminogen activator inhibitor-1 promotes angiogenesis by stimulating endothelial cell migration toward fibronectin. *Cancer Res.* **61**, 5587–5594
41. Devy, L., Blacher, S., Grignet-Debrus, C., Bajou, K., Masson, V., Gerard, R. D., Gils, A., Carmeliet, G., Carmeliet, P., Declerck, P. J., Noel, A., and Foidart, J. M. (2002) The pro- or antiangiogenic effect of plasminogen activator inhibitor 1 is dose dependent. *FASEB J.* **16**, 147–154
42. Oganesian, A., Armstrong, L. C., Migliorini, M. M., Strickland, D. K., and Bornstein, P. (2008) Thrombospondins use the VLDL receptor and a nonapoptotic pathway to inhibit cell division in microvascular endothelial cells. *Mol. Biol. Cell* **19**, 563–571
43. Krady, M. M., Zeng, J., Yu, J., MacLauchlan, S., Skokos, E. A., Tian, W., Bornstein, P., Sessa, W. C., and Kyriakides, T. R. (2008) Thrombospondin-2 modulates extracellular matrix remodeling during physiological angiogenesis. *Am. J. Pathol.* **173**, 879–891
44. Murakami, M., and Simons, M. (2009) Regulation of vascular integrity. *J. Mol. Med. (Berl)* **87**, 571–582
45. Davis, G. E., and Senger, D. R. (2005) Endothelial extracellular matrix: Biosynthesis, remodeling, and functions during vascular morphogenesis and neovessel stabilization. *Circ. Res.* **97**, 1093–1107
46. Blache, U., Vallmajo-Martin, Q., Horton, E. R., Guerrero, J., Djonov, V., Scherberich, A., Erler, J. T., Martin, I., Snedeker, J. G., Milleret, V., and Ehrbar, M. (2018) Notch-inducing hydrogels reveal a perivascular switch of mesenchymal stem cell fate. *EMBO Rep.* **19**, e45964
47. Patel, N. S., Li, J. L., Generali, D., Poulsom, R., Cranston, D. W., and Harris, A. L. (2005) Up-regulation of delta-like 4 ligand in human tumor vasculature and the role of basal expression in endothelial cell function. *Cancer Res.* **65**, 8690–8697
48. Tang, T., Li, L., Tang, J., Li, Y., Lin, W. Y., Martin, F., Grant, D., Solloway, M., Parker, L., Ye, W., Forrest, W., Ghilardi, N., Oravecz, T., Platt, K. A., Rice, D. S., *et al.* (2010) A mouse knockout library for secreted and transmembrane proteins. *Nat. Biotechnol.* **28**, 749–755
49. Suzuki-Inoue, K., Kato, Y., Inoue, O., Kaneko, M. K., Mishima, K., Yatomi, Y., Yamazaki, Y., Narimatsu, H., and Ozaki, Y. (2007) Involvement of the snake toxin receptor CLEC-2, in podoplanin-mediated platelet activation, by cancer cells. *J. Biol. Chem.* **282**, 25993–26001
50. Suzuki-Inoue, K., Fuller, G. L., Garcia, A., Eble, J. A., Pohlmann, S., Inoue, O., Gartner, T. K., Hughan, S. C., Pearce, A. C., Laing, G. D., Theakston, R. D., Schweighoffer, E., Zitzmann, N., Morita, T., Tybulewicz, V. L., *et al.* (2006) A novel Syk-dependent mechanism of platelet activation by the C-type lectin receptor CLEC-2. *Blood* **107**, 542–549
51. Astarita, J. L., Acton, S. E., and Turley, S. J. (2012) Podoplanin: Emerging functions in development, the immune system, and cancer. *Front. Immunol.* **3**, 283
52. Ramirez, M. I., Millien, G., Hinds, A., Cao, Y., Seldin, D. C., and Williams, M. C. (2003) T1alpha, a lung type I cell differentiation gene, is required for normal lung cell proliferation and alveolus formation at birth. *Dev. Biol.* **256**, 61–72
53. Breiteneder-Geleff, S., Soleiman, A., Kowalski, H., Horvat, R., Amann, G., Kriehuber, E., Diem, K., Weninger, W., Tschachler, E., Alitalo, K., and Kerjaschki, D. (1999) Angiosarcomas express mixed endothelial phenotypes of blood and lymphatic capillaries: Podoplanin as a specific marker for lymphatic endothelium. *Am. J. Pathol.* **154**, 385–394
54. Tsukiji, N., Inoue, O., Morimoto, M., Tatsumi, N., Nagatomo, H., Ueta, K., Shirai, T., Sasaki, T., Otake, S., Tamura, S., Tachibana, T., Okabe, M., Hirashima, M., Ozaki, Y., and Suzuki-Inoue, K. (2018) Platelets play an essential role in murine lung development through Clec-2/podoplanin interaction. *Blood* **132**, 1167–1179
55. Suzuki-Inoue, K., Inoue, O., Ding, G., Nishimura, S., Hokamura, K., Eto, K., Kashiwagi, H., Tomiyama, Y., Yatomi, Y., Umemura, K., Shin, Y., Hirashima, M., and Ozaki, Y. (2010) Essential *in vivo* roles of the C-type lectin receptor CLEC-2: Embryonic/neonatal lethality of CLEC-2-deficient mice by blood/lymphatic misconnections and impaired thrombus formation of CLEC-2-deficient platelets. *J. Biol. Chem.* **285**, 24494–24507
56. Bertozzi, C. C., Schmaier, A. A., Mericko, P., Hess, P. R., Zou, Z., Chen, M., Chen, C. Y., Xu, B., Lu, M. M., Zhou, D., Sebzda, E., Santore, M. T., Merianos, D. J., Stadtfeld, M., Flake, A. W., *et al.* (2010) Platelets regulate lymphatic vascular development through CLEC-2-SLP-76 signaling. *Blood* **116**, 661–670
57. Herzog, B. H., Fu, J., Wilson, S. J., Hess, P. R., Sen, A., McDaniel, J. M., Pan, Y., Sheng, M., Yago, T., Silasi-Mansat, R., McGee, S., May, F., Nieswandt, B., Morris, A. J., Lupu, F., *et al.* (2013) Podoplanin maintains high endothelial venule integrity by interacting with platelet CLEC-2. *Nature* **502**, 105–109
58. Farr, A. G., Berry, M. L., Kim, A., Nelson, A. J., Welch, M. P., and Aruffo, A. (1992) Characterization and cloning of a novel glycoprotein expressed by stromal cells in T-dependent areas of peripheral lymphoid tissues. *J. Exp. Med.* **176**, 1477–1482
59. Hallmann, R., Horn, N., Selg, M., Wendler, O., Pausch, F., and Sorokin, L. M. (2005) Expression and function of laminins in the embryonic and mature vasculature. *Physiol. Rev.* **85**, 979–1000
60. Stratman, A. N., Malotte, K. M., Mahan, R. D., Davis, M. J., and Davis, G. E. (2009) Pericyte recruitment during vasculogenic tube assembly stimulates endothelial basement membrane matrix formation. *Blood* **114**, 5091–5101
61. Scheppke, L., Murphy, E. A., Zarpellon, A., Hofmann, J. J., Merkulova, A., Shields, D. J., Weis, S. M., Byzova, T. V., Ruggeri, Z. M., Iruela-Arispe, M. L., and Cheresh, D. A. (2012) Notch promotes vascular maturation by inducing integrin-mediated smooth muscle cell adhesion to the endothelial basement membrane. *Blood* **119**, 2149–2158
62. Poulos, M. G., Guo, P., Kofler, N. M., Pinho, S., Gutkin, M. C., Tikhonova, A., Aifantis, I., Frenette, P. S., Kitajewski, J., Rafii, S., and Butler, J. M. (2013) Endothelial Jagged-1 is necessary for homeostatic and regenerative hematopoiesis. *Cell Rep.* **4**, 1022–1034
63. Liu, H., Kennard, S., and Lilly, B. (2009) NOTCH3 expression is induced in mural cells through an autoregulatory loop that requires endothelial-expressed JAGGED1. *Circ. Res.* **104**, 466–475
64. Jin, S., Hansson, E. M., Tikka, S., Lanner, F., Sahlgren, C., Farnebo, F., Baumann, M., Kalimo, H., and Lendahl, U. (2008) Notch signaling regulates platelet-derived growth factor receptor-beta expression in vascular smooth muscle cells. *Circ. Res.* **102**, 1483–1491
65. High, F. A., Lu, M. M., Pear, W. S., Loomes, K. M., Kaestner, K. H., and Epstein, J. A. (2008) Endothelial expression of the Notch ligand Jagged1 is required for vascular smooth muscle development. *Proc. Natl. Acad. Sci. U. S. A.* **105**, 1955–1959
66. Xue, Y., Gao, X., Lindsell, C. E., Norton, C. R., Chang, B., Hicks, C., Gendron-Maguire, M., Rand, E. B., Weinmaster, G., and Gridley, T. (1999) Embryonic lethality and vascular defects in mice lacking the Notch ligand Jagged1. *Hum. Mol. Genet.* **8**, 723–730
67. Limbourg, F. P., Takeshita, K., Radtke, F., Bronson, R. T., Chin, M. T., and Liao, J. K. (2005) Essential role of endothelial Notch1 in angiogenesis. *Circulation* **111**, 1826–1832
68. Krebs, L. T., Shutter, J. R., Tanigaki, K., Honjo, T., Stark, K. L., and Gridley, T. (2004) Haploinsufficient lethality and formation of arteriovenous malformations in Notch pathway mutants. *Genes Dev.* **18**, 2469–2473
69. Huppert, S. S., Le, A., Schroeter, E. H., Mumm, J. S., Saxena, M. T., Milner, L. A., and Kopan, R. (2000) Embryonic lethality in mice homozygous for a processing-deficient allele of Notch1. *Nature* **405**, 966–970
70. Gale, N. W., Dominguez, M. G., Noguera, I., Pan, L., Hughes, V., Valenzuela, D. M., Murphy, A. J., Adams, N. C., Lin, H. C., Holash, J., Thurston, G., and Yancopoulos, G. D. (2004) Haploinsufficiency of delta-like 4 ligand results in embryonic lethality due to major defects in arterial and vascular development. *Proc. Natl. Acad. Sci. U. S. A.* **101**, 15949–15954